

# **Mass and heat transfer limitations in open cell foams for the catalytic methane combustion in lean conditions.**

**Politecnico di Torino.**

**2018-2019**

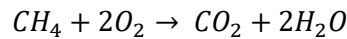
## Index

1. Introduction.....	4
2. Experimental Section.....	5
2.1. Chemicals and Foams .....	5
2.2 Catalysts Preparation .....	5
3. Estimation of fluid properties .....	6
4. Foam parameters .....	9
5. Estimation of dimensionless numbers .....	10
6. Kinetic reaction estimation .....	11
7. Evaluation of External and Internal Mass Transfer Limitations. ....	12
8. Evaluation of External Interphase (Gas-Solid) and Internal Heat Transfer Limitations .....	14
9. Resistance to mass transfer .....	14
10. Resistance to heat transfer .....	16
11. Results .....	19
11.1. Influence of temperature and space velocity on catalytic activity .....	19
11.2. Kinetic.....	20
11.3. Evaluation of external and internal mass transfer .....	21
11.3.1. Da-I .....	21
11.3.2. Da-II .....	22
11.3.3. Da-III .....	24
11.3.4. Ca.....	25
11.3.5. WP .....	26
11.4. Evaluation external and internal heat transfer.....	27
11.5. Resistance to mass transfer .....	28
11.5.1. Resistance Vs. Temperature.....	28
11.5.2. Concentration ratios Vs. Temperature.....	30
11.5.3. <i>Shapp</i> Vs. $\frac{1}{T}$ .....	32
11.5.4. External, internal or reaction resistance/ total resistance ratio Vs. Temperature. ....	34
11.5.5. Effectiveness factor Vs. Modulus Thiele. ....	36
11.6. Resistance to heat transfer .....	38
11.6.1 Heat transfer resistance Vs. Temperature .....	38
11.6.2. Peclet numbers Vs. external resistance/total resistance ratio .....	40
11.6.3. Peclet numbers Vs. internal resistance/total resistance ratio .....	42

11.7.	Estimation of mass transfer coefficient. ....	44
12.	Conclusion .....	45
13.	Bibliography.....	46

## 1. Introduction

The present work is about the behavior of methane in open cell foam. As it knows, methane is one of greenhouse gasses (GHG) the rest are carbon dioxide, nitrous oxide and chlorofluorocarbons. GHG emissions at atmosphere lead to the increase of the earth's temperature. Methane is emitted during the production and transport of coal, natural gas and oil. And methane emissions also come from livestock and other agricultural practices and by the decay of organic waste in municipal solid waste landfills. Methane is the second most powerful GHG, it contributes 16% to the overall GHG emissions. One characteristic of methane emissions is its low concentration, usually 1% or lower. In this study will be analyzed 1% and 0.5% methane combustion reaction. This combustion process consists on an exothermic reaction between methane and oxygen in the air. When this reaction takes place, the result is carbon dioxide (CO<sub>2</sub>), water and a great amount of energy. The following reaction represents the combustion of methane in lean conditions, it is meaning, low temperature and methane concentration and excess O<sub>2</sub> concentration.



Open cell foams (OCF) are used technologies to mitigate methane emissions. These are about macroporous reticulated three-dimensional (3D) structures in which the cells are connected by open windows, providing high porosity from 0.78 to 0.72. OCFs provide advantages compared to packed bed reactors, such as reduced pressure drops, high specific surface area, enhanced heat transfer, and high mechanical strength. These characteristics allow to work at high space velocity as 90 WHSV. However, disadvantages of OCFs are that the catalytic layer needs to be highly active and stable, as well as resistant to thermal and mechanical stresses [2]. And the lack of information about these structures due to this technology is quite new. From the point industrial vision OCFs are widely used in environmental applications for controlling both automotive and stationary emissions. The OCF material used in this research is zirconia. <sup>[1]</sup>

The cobalt oxide catalyst was prepared by solution combustion synthesis (SCS), using glycine as a precursor. This spinel structure has some interesting physical and chemical properties And Pd-doped catalyst were prepared by the incipient wetness impregnation (IWI). The SCS is a technique being investigated so far to create materials with enhanced catalytic properties. It essentially means decomposing a material in the presence of a reducing agent (organic fuel as glycine) to create new structures with different properties through a redox reaction. The reaction involved in the SCS generates a significant volume of high-purity foamy elements because of the exothermicity of the redox reaction. <sup>[3]</sup>  
Advantages of SCS: <sup>[4]</sup>

1. Use of relatively simple equipment
2. Use of relatively cheap reactants (like nitrates)
3. Exothermic, fast and self-sustaining reaction
4. Formation of high purity products with various size and shape
5. Adaptability to covering processes on various structured substrates via in situ SCS.

[5] The IWI has been successfully used in the synthesis of highly dispersed catalysts of noble metals, such as Pt, Rh, Pd or Ru. In this technique the active metal precursor is dissolved in an aqueous or organic solution, and the solution is added to a catalyst support containing the same pore volume as the volume of the solution that was added. The catalyst can then be dried and calcined to drive off the volatile components within the solution, depositing the metal on the catalyst surface.

## 2. Experimental Section

In this section, the steps followed in the laboratory are briefly explained and the chemicals used.

### 2.1. Chemicals and Foams

Chemicals Cobalt (II) nitrate hexahydrate  $\text{Co}(\text{NO}_3)_2 \cdot 6\text{H}_2\text{O}$  ( $\geq 98\%$  purity), palladium(II) nitrate hydrate  $\text{Pd}(\text{NO}_3)_2 \cdot x\text{H}_2\text{O}$  ( $\geq 99\%$  purity), and glycine  $\text{NH}_2\text{CH}_2\text{COOH}$  ( $\geq 99\%$  purity) were purchased from Sigma-Aldrich. Aqueous solutions were prepared using ultrapure water obtained from a Millipore Milli-Q system with a resistivity  $> 18 \text{ M}\Omega\text{cm}^{-1}$ . Pure methane, oxygen, and nitrogen gases (purity 99.999%) were supplied in cylinders provided by SIAD company and used as received. <sup>[1]</sup>

### 2.2 Catalysts Preparation

In order to obtain the catalytic coating of OCF, it will follow these steps, where it explains what it needs to do in each technique (SCS and IWI) to finally achieve 100 mg of  $\text{Co}_3\text{O}_4$  and 3% of Pd. Everything must be repeated for 150 and 250 mg catalyst loading.

Firstly, the dissolution is prepared, for that purpose 500 mg of Cobalt (II) nitrate hexahydrate and 250 mg of glycine have been weighed in analytical balance. These compounds are mixed with distilled water. Finally, the dissolution is left for 2 hours at  $50^\circ\text{C}$  in hot plate with magnetic agitation and thus achieve the dissolution well mixed.

Secondly, the structure is weighted without catalyst and next it is immersed in the dissolution for 2 or 3 minutes. Now the Synthesis Combustion starts, the OCF is put in furnace for 15 minutes at  $250^\circ\text{C}$  and after it is weighted to know how much catalyst has adhered to the structure. The last steps must repeat them until it obtains 100 mg of cobalt oxide.

After that the calcination begins, where the structure is left for 4 hours at  $600^\circ\text{C}$  in the furnace.

Finally, the last step starts, in which it is used the technique of incipient wetness impregnation (IWI). For it, it is prepared a solution of palladium nitrate and it puts in the plate with magnetic agitation for 2 hours, this time without heat to prevent water from evaporating. Once the dissolution is well mixed, the foam is immersed in it. And it places in the furnace at  $140^\circ\text{C}$  for 10 minutes. The latter must be repeated until 3% of palladium is adhered to the structure. And finally, the foam is put in calcination at  $600^\circ\text{C}$  for 4 hours.

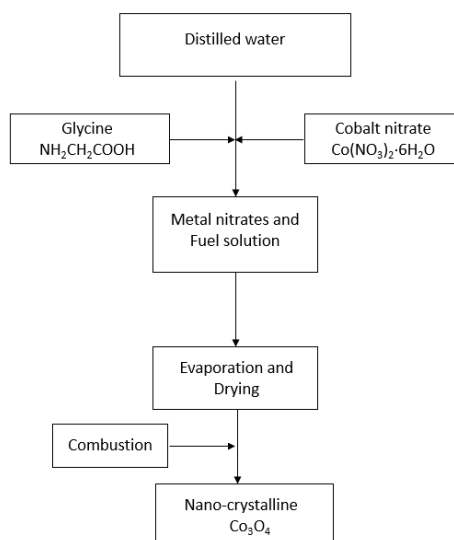


Figure 1: A schematic representation of the synthesis process.

### 3. Estimation of fluid properties

The different properties of the gas mixture were calculated by following equations:

1) *Molecular weight*

$$M_{mix} = \sum_{i=1}^n y_i M_i \quad (1)$$

2) *Density*

$$\rho_{mix} = \frac{P M_{mix}}{R T} \quad (2)$$

3) *Viscosity* <sup>[6]</sup>

Firstly, it has estimated the value of the viscosity of CH<sub>4</sub>, O<sub>2</sub>, H<sub>2</sub>O, CO<sub>2</sub> for each temperature in range from 100°C to 700°C by this equation:

$$\mu = 2.6693 \cdot 10^{-6} \frac{(MT)^{0.5}}{\sigma^2 \Omega_\mu} \quad (3)$$

Where M is the molecular weight of each component (g/mol), T is the temperature (k),  $\sigma$  is the collision diameter (Å) and  $\Omega_\mu$  is the collision integral (-). Below are two tables with  $\sigma$  and  $\Omega_\mu$  values.

**Table 1:** Lennard-Jones parameters for each component.

Component	$\sigma$ (Å)	$\frac{\epsilon}{k}$
CH <sub>4</sub>	3.758	148.6
O <sub>2</sub>	3.467	106.7
CO <sub>2</sub>	3.941	195.2
H <sub>2</sub> O	2.649	356
N <sub>2</sub>	3.798	71.4

The collision integral (Table 2) can be consulted in function of dimensionless temperature ( $T^*$ ) definite as,

$$T^* = \frac{k T}{\epsilon} \quad (4)$$

**Table 2:** Collision integral value

$T^*$	$\Omega_{\mu}$	$T^*$	$\Omega_{\mu}$	$T^*$	$\Omega_{\mu}$	$T^*$	$\Omega_{\mu}$
0.25	3.0353	1.30	1.4000	2.7	1.0700	4.8	0.9326
0.30	2.8458	1.35	1.3760	2.8	1.0591	4.9	0.9288
0.35	2.6791	1.40	1.3538	2.9	1.0489	5.0	0.9252
0.40	2.5316	1.45	1.3331	3.0	1.0394	6.0	0.8948
0.45	2.4003	1.50	1.3139	3.1	1.0304	7.0	0.8719
0.50	2.2831	1.55	1.2959	3.2	1.0220	8.0	0.8535
0.55	2.1781	1.60	1.2791	3.3	1.0141	9.0	0.8382
0.60	2.0839	1.65	1.2633	3.4	1.0066	10	0.8249
0.65	1.9991	1.70	1.2486	3.5	0.9995	12	0.8026
0.70	1.9226	1.75	1.2347	3.6	0.9927	14	0.7844
0.75	1.8535	1.80	1.2216	3.7	0.9864	16	0.7690
0.80	1.7909	1.85	1.2092	3.8	0.9803	18	0.7556
0.85	1.7341	1.90	1.1975	3.9	0.9745	20	0.7439
0.90	1.6825	1.95	1.1865	4.0	0.9690	25	0.7196
0.95	1.6354	2.00	1.1760	4.1	0.9637	30	0.7003
1.00	1.5925	2.1	1.1565	4.2	0.9587	35	0.6844
1.05	1.5533	2.2	1.1388	4.3	0.9539	40	0.6710
1.10	1.5173	2.3	1.1227	4.4	0.9493	50	0.6491
1.15	1.4843	2.4	1.1079	4.5	0.9448	75	0.6111
1.20	1.4539	2.5	1.0943	4.6	0.9406	100	0.5855
1.25	1.4259	2.6	1.0817	4.7	0.9365	150	0.5512

Once the values were achieved it was estimated viscosity of the mixture by following equation

$$\mu_{mix} = \frac{\sum_{i=1}^n \mu_i y_i M_i^{\frac{1}{2}}}{\sum_{i=1}^n y_i M_i^{\frac{1}{2}}} \quad (5)$$

#### 4) Diffusivity<sup>[7]</sup>

Fuller equation has used to determine binary gasses diffusivities CH<sub>4</sub>, O<sub>2</sub>, CO<sub>2</sub>, H<sub>2</sub>O and N<sub>2</sub>.

$$D_{AB} = \frac{0.001T^{1.75} \left( \frac{1}{M_A} + \frac{1}{M_B} \right)^{0.5}}{P \left[ (\sum V_A)^{\frac{1}{3}} + (\sum V_B)^{\frac{1}{3}} \right]^2} \quad (6)$$

Where P is the total pressure (atm), M<sub>i</sub> is the molecular weight (g/mol), D<sub>AB</sub> is the diffusivity (cm<sup>2</sup>/s) and  $\sum V_i$  is sum of the diffusion volume for component i, as given in Table 3.

**Table 3:** Special atomic diffusion volumes

Component	V <sub>i</sub> (cm <sup>3</sup> ·mol <sup>-1</sup> )
CH <sub>4</sub>	24,42
O <sub>2</sub>	16,6
CO <sub>2</sub>	26,9
H <sub>2</sub> O	12,7
N <sub>2</sub>	17,9

Diffusivity of CH<sub>4</sub> in gas phase ( $D_{CH_4}$ ) was calculated from the binary diffusion of CH<sub>4</sub> and i gas species

( $D_{CH_4-i}$ ) by:

$$D_{CH_4 \text{ mix}} = \frac{1 - y_{CH_4}}{\sum_{i=1; i \neq CH_4}^n \frac{y_i}{D_{CH_4-i}}} \quad (7)$$

5) *Specific heat transfer* [8]

Specific heat transfer of each component was determined by the following relationships:

$$Cp_{CH_4} = 5.34 + 0.0115T \quad (8)$$

$$Cp_{O_2} = 8.27 + 0.000258T - \frac{187700}{T^2} \quad (9)$$

$$Cp_{CO_2} = 10.34 + 0.00247T - \frac{195500}{T^2} \quad (10)$$

$$Cp_{H_2O} = 8.22 + 0.00015T + 0.00000134T^2 \quad (11)$$

$$Cp_{N_2} = 6.5 + 0.001T \quad (12)$$

And Cp of the gas mixture by

$$Cp_{mix} = \sum_{i=1}^n y_i Cp_i \quad (13)$$

6) *Thermal conductivity* [8]

For methane and cyclic compounds below reduced temperatures of 1.0:

$$k_G = 4.45 \cdot 10^{-7} \frac{T}{T_c} \frac{Cp}{T_c^{\frac{1}{6}} M^{\frac{1}{2}} \left( \frac{101325}{P_c} \right)^{\frac{2}{3}}} \quad (14)$$

For these hydrocarbons above reduced temperatures of 1.0 and for other hydrocarbons at any temperature:

$$k_G = 10^{-7} (14.52T_r - 5.14)^{\frac{2}{3}} \frac{Cp}{T_c^{\frac{1}{6}} M^{\frac{1}{2}} \left( \frac{101325}{P_c} \right)^{\frac{2}{3}}} \quad (15)$$

where  $k_G$  is the vapor thermal conductivity (W/m K),  $T_r$  is the reduced temperature  $T_r = \frac{T}{T_c}$ ,  $T$  is the temperature (K),  $T_c$  is the critical temperature (K),  $Cp$  is the heat capacity at constant pressure (J/kmol K),  $M$  is the molecular weight and  $P_c$  is the critical pressure (kPa).

The component properties ( $T_c$  and  $P_c$ ) are indicated on the table 4.

Table 4: Component properties.

Component	M [g/mol]	$T_c$ [K]	$P_c$ [kPa]
CH <sub>4</sub>	16.043	190.4	4600
O <sub>2</sub>	31.99	154.6	5040
CO <sub>2</sub>	44.01	304.1	7380
H <sub>2</sub> O	18.016	647.3	22120
N <sub>2</sub>	28.0134	126.2	3390

Finally,  $k_{mix}$  was calculated as follow:

$$k_{mix} = \frac{\sum_{i=1}^n k_i y_i M_i^{\frac{1}{3}}}{\sum_{i=1}^n y_i M_i^{\frac{1}{3}}} \quad (16)$$

#### 4. Foam parameters

Before to obtain the dimensionless numbers, it is necessary to estimate foam parameters. Firstly, it shows the equations to be able to estimate parameters and then, on table 5 the corresponding values for each catalytic loading (100 mg, 150 mg and 250 mg).

$$d_{p,c} \text{ (average coated pore diameter)} \quad d_{p,c} = d_p - 2 c_t \quad (17)$$

$$d_{f,c} \text{ (average coated face diameter)} \quad d_{f,c} = d_f + 2 c_t \quad (18)$$

$$t_s \text{ (average strut dimension)} \quad t_s = t_{s,o} + 2 c_t \quad (19)$$

$$d_f \text{ (face diameter)} \quad d_f = d_p + t_s \quad (20)$$

$$\rho_r \text{ (foam relative density)} \quad \rho_r = \frac{\rho_f}{\rho_{solid}} = 2.59 \left( \frac{t_s}{d_f} \right)^2 \quad (21)$$

$$S_{ag} \text{ (geometric surface area)} \quad S_{ag} = \frac{4.82}{d_f} \sqrt{\rho_r} \quad (22)$$

$$S_a \text{ (calculated surface area)} \quad S_a = V_{OCF} \cdot S_{ag} \quad (23)$$

$$\varepsilon \text{ (voidage)} \quad \varepsilon = 1 - \rho_r \quad (24)$$

$$\tau \text{ (tortuosity)} \quad \tau = 1 + \phi \frac{[1 - 0.971(1 - \varepsilon_0)^{0.5}]}{4\varepsilon_0(1 - \varepsilon_0)^{0.5}} (1 - \varepsilon_0) \quad (25)$$

$$c_t \text{ (catalyst thickness)} \quad c_t = \frac{m_{cat}}{S_a \cdot \rho_{cat}} \quad (26)$$

$$c_{load} \text{ (catalyst loading)} \quad c_{load} = \frac{m_{cat}}{S_a} \quad (27)$$

**Table 5:** Foam parameters

	$d_{OCF}$ [mm]	9	$L_{OCF}$ [mm]	30	
	$\rho_{cat}$ [mg/mm <sup>3</sup> ]	2	$V_{OCF}$ [mm <sup>3</sup> ]	1908,52	
$m_{Co3O4}$	[mg]	0	<b>100</b>	<b>150</b>	<b>250</b>
$m_{Pd\ 3\%}$	[mg]	0	3	4,5	7,5
$m_{cat}$	[mg]	0	103	154,5	257,5
$d_{p,c}$	[mm]	1,30	1,25	1,23	1,18
$t_s$	[mm]	0,47	0,52	0,54	0,59
$d_f$	[mm]	1,77	1,77	1,77	1,77
$\rho_r$	-	0,18	0,22	0,24	0,28
$Sag$	[mm <sup>-1</sup> ]	1,16	1,28	1,34	1,45
$Sa$	[mm <sup>2</sup> ]	2220,98	2440,13	2549,70	2768,85
$\epsilon$	-	0,82	0,78	0,76	0,72
$\tau$	-	1,37	1,40	1,41	1,44
$c_t$	[mm]	0	0,02	0,03	0,06
$C_{load}$	[mg/mm <sup>2</sup> ]	0	0,05	0,07	0,12
$d_{f,c}$	[mm]	0	1,82	1,84	1,89

## 5. Estimation of dimensionless numbers

### 1) Schmidt

$$Sc = \frac{\mu_{mix}}{\rho_{mix} D_{CH_4}} \quad (28)$$

### 2) Reynold

$$Re = \frac{d_{p,c} u \rho_{mix}}{\mu_{mix}} \quad (29)$$

### 3) Sherwood

Due to the lack of information on correlations to calculate the Sherwood number 3 different equations have been searched to obtain the Sherwood and be able to estimate a new correlation based on the previous data.

$$A. \quad Sh = 0,43Re^{0,446}Sc^{0,33} \quad (30) \quad \text{for} \quad 5 < Re < 50 \quad [9]$$

$$B. \quad Sh = 1,00 Re^{0,47} Sc^{0,33} \left( \frac{d_{f,c}}{0,001m} \right)^{0,58} \epsilon^{0,44} \quad (31) \quad [2]$$

$$C. \quad Sh_{ds,avg} = \epsilon^{-2} (0,566Re_{ds,avg}^{0,33} + 0,039Re_{ds,avg}^{0,8}) Sc^{\frac{1}{3}} \quad (32) \quad [10]$$

The applicability ranges of the hereby derived correlation are:

$$1 < Re_{ds,avg} < 300$$

$$0.7 < \varepsilon_H < 0.95$$

$$0.3 < d_c < 5 \text{ mm}$$

To determine Sherwood number:

First it was assumed that the strut diameter for foams was circular and it calculated through follow equation,

$$\frac{-0.3985d_s^{c3} + 2.8803d_s^{c2}d_c + 0.2172d_s^c d_c^2 + 0.00708d_c^3}{0.419(d_c + d_s^c)^3} = 1 - \varepsilon \quad (33)$$

Where  $d_s^c$  is the circular strut diameter and  $d_c$  (is the same as  $d_f$ ) is the cell diameter.

Struts are characterized by a parabolic profile along the axis, which introduces a longitudinal variation of the strut diameter.

Thus, it was introduced an average strut diameter, calculated as the integral average of the strut diameter over its length. This quantity was estimated according to the equation for circular.

$$d_{s,avg}^c = 0.965d_s^c + 0.0314d_c \quad (34)$$

**Table 6:** circular strut diameter for each catalyst loading.

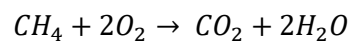
$m_{C_03O_4}$ (mg)	100	150	250
$d_{s,avg}^c$ (mm)	0,3915	0,4184	0,4775

Also, it must calculate another Reynold because it depends the  $d_{s,avg}^c$ , so the new equation is

$$Re = \frac{d_{s,avg}^c u \rho_{mix}}{\mu_{mix}} \quad (35)$$

## 6. Kinetic reaction estimation

In this part of the work, it is going to analyze kinetic of the reaction. Here, it is showed the first order methane combustion reaction, where methane is the limiting reagent.



It is going to estimated activation energy and first order reaction rate. For that it is realized a mass balance to methane

$$-r_{CH_4} = \frac{-dC_{CH_4}}{dt} = kC_{CH_4}$$

$$\int_{C_{CH_4,0}}^{C_{CH_4,f}} \frac{-dC_{CH_4}}{C_{CH_4}} = \int_0^\tau k dt$$

$$k^{obs} = \frac{1}{\tau} \ln \left( \frac{1}{1 - X_{CH_4}} \right)$$

Where  $\tau$  is the residence time and It is calculated by following equation

$$\tau = \frac{W \cdot C_{CH_4,o}}{F_{CH_4,in}} \quad (36)$$

Being  $W$  catalyst weight [g],  $C_{CH_4,o}$  initial concentration [kmol/m<sup>3</sup>] and  $F_{CH_4,in}$  inlet total flux [kmol/s].

In order to be able to obtain  $E_a$  and  $k^r$  it is used Arrhenius equation

$$k^r = k_o \exp \left( \frac{-E_a}{RT} \right) \quad (37)$$

## 7. Evaluation of External and Internal Mass Transfer Limitations.

The tortuous nature of the OCFs structures allows high contact efficiency between reactants and catalyst. However, mass transfer limitations can still occur with strong impact on the catalytic performance. The catalytic reaction between reactant molecules and active sites, generally located inside the catalyst pores, takes place after the reactant molecules diffuse from gas phase to the catalyst surface (external diffusion) and through the pores of the coated layer (internal diffusion). Thus, three operating regimes, namely kinetic, external mass transfer and internal diffusion, can control the processes.

The characteristic time analysis is widely used to investigate physical and chemical processes involved in structured catalysts. For this analysis have been estimated these different times.

1. *Residence time* ( $t_c$ ): describes the flow time of reactants through the OCFs catalysts at feed inlet conditions. It was calculated by,

$$t_c = \frac{L \cdot \tau}{u} \quad (38)$$

where  $L$  is the OCF length,  $u$  is the inlet gas velocity and  $\tau$  is the tortuosity of the OCF.

2. *External mass transfer time* ( $t_{ext}$ ): involves the diffusion of methane from bulk gas to the catalyst surface. It was calculated by,

$$t_{ext} = \frac{d_{p,c}^2}{4 D_{CH_4} Sh} \quad (39)$$

where  $d_{p,c}$  is the average coated pore diameter,  $D_{CH_4}$  is the diffusivity of CH<sub>4</sub> in gas phase and  $Sh$  is the Sherwood number.

3. *Coated layer diffusion time* ( $t_{int}$ ): involves the transport of reactants inside the pores of the catalytic layer. It was calculated by,

$$t_{int} = \frac{c_t^2}{D_{CH_4,e}} \quad (40)$$

where  $c_t$  is the coated layer thickness and  $D_{CH_4,e}$  is the effective diffusivity of CH<sub>4</sub> in the coated layer.

4. *Reaction time* ( $t_r$ ): describes the rate of methane conversion. It was calculated by,

$$t_r = \frac{C_{CH_4}}{r_{CH_4} \rho_c} \quad (41)$$

Where  $C_{CH_4}$  is the concentration of methane in the feed mixture,  $r_{CH_4}$  is the observed reaction rate with respect to methane and  $\rho_c$  is the density of the catalytic layer.

Damköhler numbers were determined to describe the trade-off between reaction kinetic and diffusion limitations. They are the following:

1. *First Damköhler number (Da-I)*: Relates the residence time and the reaction time. It means that when Da-I is greater than 1 the mixture has sufficient time to react over the catalyst within OCFs pores. It was calculated by,

$$Da - I = \frac{t_c}{t_r} > 1 \quad (42)$$

2. *Second Damköhler number (Da-II)*: Relates the external mass transfer and the reaction time. It means that when Da-II is greater than 0,1 external mass transfer become important in the system. It was calculated by,

$$Da - II = \frac{t_{ext}}{t_r} < 0.1 \quad (43)$$

3. *Third Damköhler number (Da-III)*: Relates coated layer diffusion time and reaction time and allows to determine the internal mass transfer limitations. When it is lower than 1, reactants rapidly diffuse through the pores of the coated layer, avoiding the formation of concentration gradients between the catalyst surface and active sites. It was calculated by,

$$Da - III = \frac{t_{int}}{t_r} < 1 \quad (44)$$

To confirm these results (Damköhler Numbers) it has also calculated Carberry and Weisz-Prater numbers. Where the effect of external mass transfer limitation was determined by Carberry number (Ca) for a first-order reaction with respect to methane.

$$Ca = \frac{R_{CH_4}}{k_G GSA C_{CH_4}} < 0.05 \quad (45)$$

And internal mass transfer by Weisz-Prater number (WP)

$$WP = \frac{r_{CH_4} \rho_c C_t^2}{D_{CH_4,e} C_{CH_4,s}} < 1 \quad (46)$$

where  $CH_4$  concentration at catalyst surface ( $C_{CH_4,s}$ ) was equal to the  $CH_4$  concentration in feed mixture ( $C_{CH_4}$ ) in absence of external diffusion controlling regime, otherwise it was calculated by: <sup>[2]</sup>

$$C_{CH_4,s} = C_{CH_4} (1 - Ca) \quad (47)$$

## 8. Evaluation of External Interphase (Gas-Solid) and Internal Heat Transfer Limitations

As in section 7 it will be analyzed heat transfer limitations because of temperature profiles can be developed around the catalytic coating and inside the catalyst particles, since the reactants are consumed, and the heat can be produced or consumed during reaction.

The criterion proposed by Mears was used to test the significance of external interphase (gas-solid) heat transport limitations: <sup>[2]</sup>

$$\frac{E_a (-\Delta H_r^\circ) R_{CH_4}}{h S_{ag} R T^2} < 0.15 \quad (48)$$

And the Anderson criterion to internal heat transfer limitations:

$$\frac{E_a (-\Delta H_r^\circ) r_{CH_4} \rho_{cat} c_t^2}{k_{wc} R T^2} < 0.75 \quad (49)$$

The enthalpy of reaction is the following,

$$\Delta H_r^\circ = -802.3 \frac{Kj}{molCH_4} \quad [11]$$

## 9. Resistance to mass transfer

For the case of a single exothermic reaction carried out in an OCF operated a low temperature (T=100C) the reaction rate is typically much lower than the external mass transport rate. This operating regime is usually referred to as the kinetic regime, where the external and internal mass transfer resistance are negligible and the observed rate is limited by kinetics. As the operating temperature increases, the reaction rate increases rapidly this increase is exponential with temperature (Arrhenius dependence). However, since the diffusivities of the reacting species in the gas phase and washcoat are weak functions of temperature, the external and internal mass transfer rates increase, only slightly with temperature. Thus, at high operating temperatures, the resistance due to reaction becomes negligible and the main resistance is due to external and internal mass transfer (washcoat diffusion). It refers to this transition regime as the combined (pore diffusion and external) mass transfer controlled regime.

Finally, at sufficiently high temperatures, the reaction is confined to a very thin boundary layer near the fluid-washcoat interface and the resistance due to pore diffusion as well as chemical reaction becomes negligible. This regime is referred to as the external mass transfer-controlled regime.

The process of overall mass transfer in an OCF is simplified by dividing to process into two parts: external mass transfer from bulk fluid phase to washcoat and internal mass transfer with chemical reaction in the washcoat.

### **External ( $Sh_e$ ) and internal ( $Sh_i$ ) mass transfer coefficient:**

External mass transfer coefficient is widely used to simplify mathematical models of convection with diffusion and reaction. It is assumed that the whole resistance for mass transfer is found in a fictitious thin film in which concentration variation happens. For internal mass transfer coefficient is used a similar model to external mass transfer, where the process of diffusion and reaction in a catalyst particle is simplified to a hypothetical film, named washcoat.

Before to obtain the values of  $Sh_e$  and  $Sh_i$  for each temperature it is necessary to calculate the following parameters:

Firstly, it is assumed that channel and washcoat shapes are circular. In the figure 2 below is shown two different radii where  $R_1$  is the channel with catalyst and  $R_2$  without catalyst,

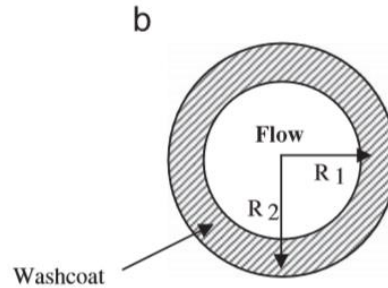


**Figure 2:** Circular channel with its two different radii.

And then it is calculated  $R_{\Omega 1}$  and  $R_{\Omega 2}$  which are characteristic length scales for transverse diffusion associated with fluid phase and washcoat, respectively with the following equations:

$$R_{\Omega 2} = \frac{(R_2^2 - R_1^2)}{2R_1} \quad (50)$$

$$R_{\Omega 1} = \frac{R_1}{2} \quad (51)$$

In the table 7 below the values of the parameters explained above for each catalyst load are shown

**Table 7:**

$\text{Co}_3\text{O}_4$ [mg]	100	150	250
$R_1$ [mm]	0.6268	0.6152	0.592
$R_2$ [mm]	0.65	0.65	0.65
$R_{\Omega 1}$ [mm]	0.3134	0.3076	0.296
$R_{\Omega 2}$ [mm]	0.02361	0.03576	0.0608

Estimation of internal Sherwood number ( $Sh_i$ ):

This correlation which relating to the internal Sherwood number to the Thiele modulus.

$$Sh_i = Sh_{i\infty} + \frac{\Lambda \phi^2}{1 + \Lambda \phi} \quad (52)$$

Where  $Sh_{i\infty}$  depends on washcoat geometric shape,  $\Lambda$  depends on washcoat geometric shape and kinetic parameters for this work have been used the following values  $Sh_{i\infty} = 3.0125$  and  $\Lambda = 0.38$ . And finally,  $\phi$  is the Thiele modulus which for a first order reaction is defined as which for a first order reaction is defined as

$$\phi^2 = \frac{kR_{\Omega 2}^2}{De} \quad (53)$$

Where  $k$  is the first order reaction rate and  $D_e$  is the effective diffusivity.

And the effectiveness factor:

$$\eta = \frac{1}{1 + \frac{\phi^2}{Sh_i}} \quad (53)$$

Estimation of external Sherwood number ( $Sh_e$ ):<sup>[13]</sup>

$$Sh_e(L) = Sh_{e\infty} + \frac{2.8}{Sc^{1/6}} \sqrt{P} \quad (54)$$

Where Sc is the Schmidt number,  $Sh_{e\infty} = 3.656$  [12] and P is the transverse Peclet number

$$P = \frac{R_{\Omega^1}^2 u}{D_f L} \quad (55)$$

In this equation u is the average gas velocity in the channel (m/s), Df is the molecular diffusivity (m<sup>2</sup>/s) and L is the length of the OCF (m) respectively.

Once it is obtained the results of  $Sh_i$  and  $Sh_e$ , It proceeds to estimate the overall resistance for mass transfer ( $R_t$ ). It comprises three resistance in series: fluid phase film resistance ( $R_e$ ), internal mass transfer resistance ( $R_w$ ) and reaction resistance ( $R_r$ ). These are given by the following expressions:<sup>[12]</sup>

$$R_e = \frac{1}{k_{me}} = \frac{4R_{\Omega^1}}{Sh_e(L)D_f} \quad (56)$$

$$R_w = \frac{1}{k_{mi}} = \frac{R_{\Omega^2}}{Sh_i D_e} \quad (57)$$

$$R_r = \frac{1}{kR_{\Omega^2}} \quad (58)$$

$$R_t = \frac{1}{k_{mapp}} = R_e + R_w + R_r \quad (59)$$

## 10. Resistance to heat transfer

In this section of the work it is going to analyze resistance to heat transfer. For it, are calculated various dimensionless group as it was made previously to calculate resistance to mass transfer.

As shown in the figure 3 the OCF channel is divided in three domains: flow channel ( $\Omega_f$ ), catalytic washcoat ( $\Omega_{wc}$ ) and substrate wall ( $\Omega_w$ ). The feed gas flows axially through the OCF channel while mass and heat transfer are transported in both axial and radial directions by convection and diffusion. It is distinguished between the washcoat and the substrate wall because heat is only generated in the washcoat where reactions take place.

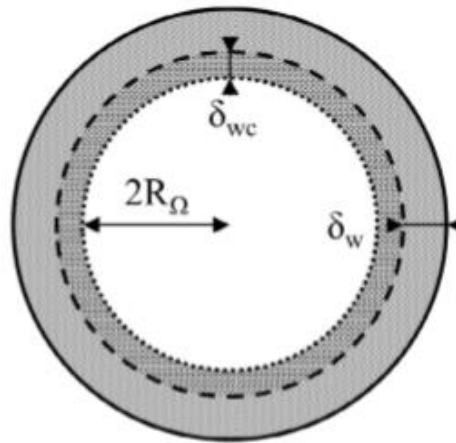


**Figure 3:** The OCF channel.

Before to estimate dimensionless numbers, it is necessary to know thermal conductivity of zirconia and cobalt oxide. As it has been difficult to find the values at each temperature, they have been graphed some values and so to get the equation that relationship between temperature and thermal conductivity. Below it is showed the plots for each oxide. <sup>[14]</sup>

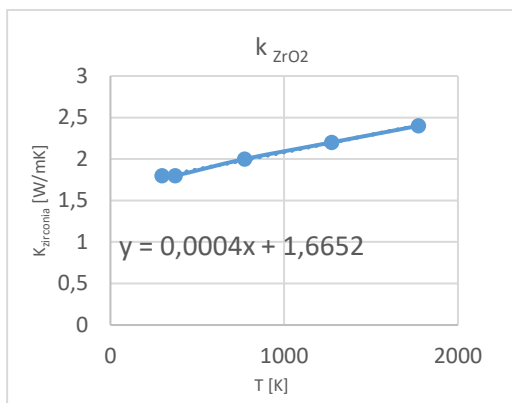


**Figure 4:** Thermal conductivity of  $ZrO_2$  <sup>[15]</sup>

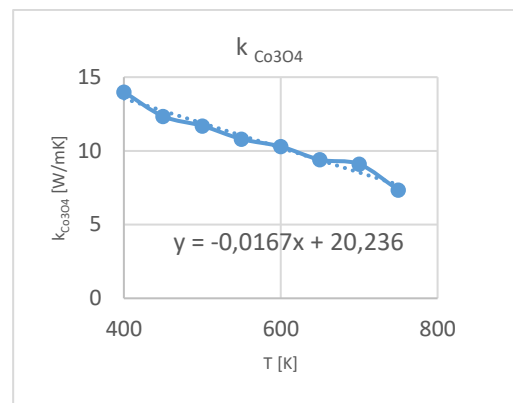


**Figure 5:** Thermal conductivity of  $Co_3O_4$  <sup>[16]</sup>

And now it is going to explain how the three different resistance are estimated: external, internal and wall.

1. *External resistance:*

In order to calculate external resistance, it is needed to estimate the following dimensionless number (Fluid Lewis number  $Le_f$ ), which depending only on the physical properties of the gas and diffusivity of the limiting reactant species.

$$Le_f = \frac{k_f}{C_p \rho D_M} \quad (60)$$

$$Nu_e = Le_f^{\frac{1}{3}} \cdot Sh_e \quad (61)$$

$$h_e = \frac{Nu_e k_M}{4R_{\Omega e}} \quad (62)$$

$$R_e^h = \frac{1}{h_e 2\pi R_{\Omega i} L} \quad (63)$$

Internal and wall resistance are directly calculated with one equation.

2. Internal resistance:

$$R_i^h = \frac{Ln\left(\frac{R_{\Omega i}}{R_{\Omega e}}\right)}{2\pi L k_{wc}} \quad (64)$$

Where  $k_{wc}$  corresponds to thermal conductivity of  $Co_3O_4$

3. Wall resistance:

$$R_w^h = \frac{Ln\left(\frac{R_w}{R_{\Omega e}}\right)}{2\pi L k_w} \quad (65)$$

Where  $k_w$  corresponds to thermal conductivity of  $ZrO_2$  and  $R_w$  is the wall diameter

$$R_w = R_{\Omega e} + c_t + t_s \quad (66)$$

$$R_t = R_e^h + R_i^h + R_w^h \quad (67)$$

The following transverse Péclet numbers (related to species and heat diffusion in the transverse direction) are described by

$$P_{m,f} = \frac{u_o R_{\Omega e}^2}{D_M L} \quad (68) \quad P_{m,wc} = \frac{u_o R_{\Omega e}^2}{D_{CH_4,e} L} \quad (69)$$

$$P_{h,f} = \frac{u_o R_{\Omega e}^2}{\alpha_f L} \quad (70) \quad P_{h,wc} = \frac{u_o R_{\Omega e}^2 k_M}{\alpha_f L k_{wc}} \quad (71) \quad P_{h,w} = \frac{u_o R_{\Omega e}^2 k_M}{\alpha_f L k_w} \quad (72)$$

Where  $\alpha_f$  is the thermal diffusivity of the fluid defined by,

$$\alpha_f = \frac{k_M}{\rho C_p} \quad (73)$$

The following axial Péclet numbers (related to heat and mass diffusion in the flow direction, washcoat and wall) are described by,

$$Pe_{m,f} = \frac{u_o L}{D_M} \quad (74) \quad Pe_{m,wc} = \frac{u_o L}{D_{CH_4,e}} \quad (75)$$

$$Pe_{h,f} = \frac{u_o L}{\alpha_f} \quad (76) \quad Pe_{h,wc} = \frac{u_o L k_M}{\alpha_f k_{wc}} \quad (77) \quad Pe_{h,w} = \frac{u_o L k_M}{\alpha_f k_w} \quad (78)$$

The subscripts  $m$  and  $h$  represent mass and heat transfer and  $f$ ,  $wc$  and  $w$  represent the flow channel, the washcoat and the substrate wall respectively.

In order to be able to calculate transverse and axial Peclet numbers for the solid phase, it is necessary to define the following parameters

$$\delta_s = t_s + c_t \quad (79)$$

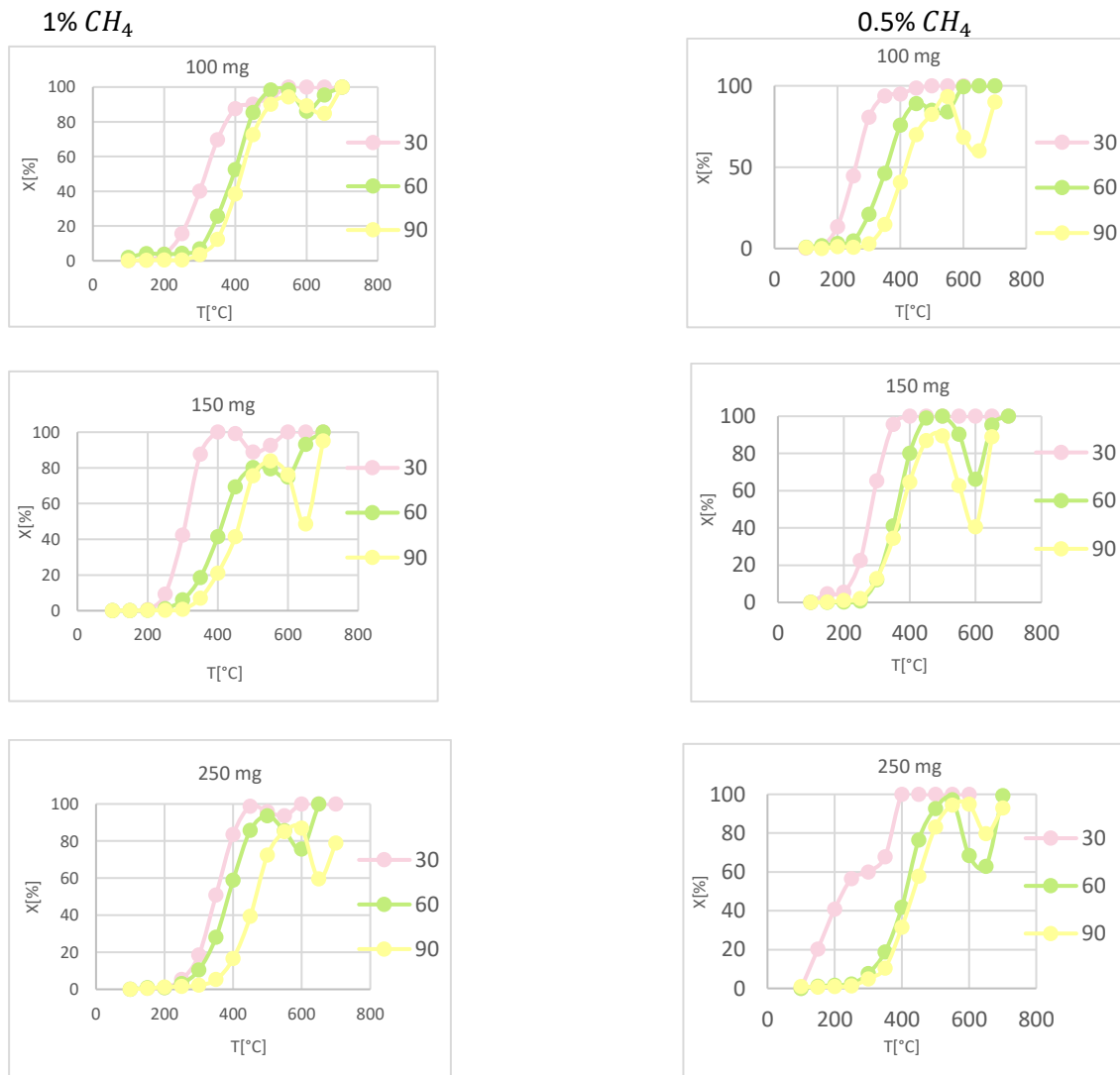
$$k_s = \frac{t_s k_w + c_t k_{wc}}{\delta_s} \quad (80)$$

$$P_{h,s} = \frac{u_o R_{\Omega e}^2 k_M}{\alpha_f L k_s} \quad (81)$$

$$Pe_{h,s} = \frac{u_o L k_M R_{\Omega e}}{\alpha_f k_s \delta_s} \quad (82)$$

## 11. Results.

### 11.1. Influence of temperature and space velocity on catalytic activity



These plots show the influence of temperature (T=100-700°C) and space velocity (WHSV=30,60 and 90) in terms of CH<sub>4</sub> conversion.

Analyzing, it is observed that total CH<sub>4</sub> conversion is reached at temperatures below 600°C and 30 WHSV in all cases, even for 0.5 % of CH<sub>4</sub> it is reached before at 400 °C. And that for 60 and 90 WHSV, it is always

produced the transformation of palladium into palladium oxide, this situation is because of there is more oxygen. Which is not good because the conversion declines. However, it doesn't always happen at 30 WHSV.

Therefore, the best fitting case is 100 mg and 30 WHSV at both methane concentrations

### 11.2. Kinetic

In this section of the work, it will discuss the kinetic, for this it is analyzed activation energy of kinetic and coated layer, calculating standard deviation with following equation,

$$\sigma = \frac{\bar{x} - x}{\bar{x}} \quad (83)$$

Where  $\sigma$  is the standard deviation,  $\bar{x}$  is the average of three values of activation energy.

As it was explained before, all parameters were obtained through Arrhenius equation.

The theoretical situation would be that, at beginning the activation energy of kinetics is the highest value. Then the activation energy of coated layer should be half of the activation energy of kinetics. And finally, activation energy tends to zero, where it is found in completely controlled mass transfer.

Below, are showed two tables 8 and 9 with the activation energy and standard deviation for each concentration of methane, respectively

**Table 8:** Kinetic for 1% CH<sub>4</sub>

<b>1% CH<sub>4</sub></b>					
	<b>WHSV</b>	<b>E<sub>kinetic</sub> [Kj/mol]</b>	<b>σ<sub>kinetic</sub></b>	<b>E<sub>coated layer</sub> [Kj/mol]</b>	<b>σ<sub>cLayer</sub></b>
<b>100 mg</b>	30	158,88	<b>0,09837539</b>	60,4	0,157366
	60	96,24	0,33478562	71,87	<b>0,002651</b>
	90	178,859	0,23657676	82,779	0,154841
<b>150 mg</b>	30	144,314	0,15731734	87,16	0,07577
	60	133,647	<b>0,07177398</b>	68,773	0,151171
	90	96,13	0,22909132	87,13	<b>0,0754</b>
<b>250 mg</b>	30	143,067	<b>0,00240566</b>	73,61	0,043529
	60	175,53	0,22395615	76,384	<b>0,007484</b>
	90	111,64	0,22154352	80,89	0,051065

**Table 9:** Kinetic of 0.5% CH<sub>4</sub>

<b>0.5% CH<sub>4</sub></b>					
	<b>WHSV</b>	<b>E<sub>kinetic</sub> [Kj/mol]</b>	<b>σ<sub>kinetic</sub></b>	<b>E<sub>coated layer</sub> [Kj/mol]</b>	<b>σ<sub>cLayer</sub></b>
<b>100 mg</b>	30	166,62	0,21278733	70,1	<b>0,01303693</b>
	60	126,9	<b>0,0763251</b>	63,23	0,10975799
	90	118,64	0,13644767	79,75	0,12282307
<b>150 mg</b>	30	143,42	0,07285539	66,86	0,09875179
	60	173,9	0,12418385	82,6	0,11341763
	90	146,76	<b>0,05126382</b>	73,1	<b>0,01463888</b>
<b>250 mg</b>	30	160,79	0,23857063	63,86	0,08119074
	60	129,08	<b>0,00569254</b>	70,082	<b>0,00833058</b>
	90	99,587	0,23287808	74,568	0,07287455

Firstly, it is started comparing 100 mg catalyst loading on different concentration of methane (1% and 0.5%). Where the best option to choose in 1% CH<sub>4</sub> is 30 WHSV for kinetic and 60 WHSV for coated layer. For 0.5% CH<sub>4</sub> is 60 WHSV for kinetic and 30 WHSV for coated layer.

Secondly, it is compared 150 mg catalyst loading on the same way as it is explained before, and the results are that for 1% CH<sub>4</sub> is 60 WHSV for kinetic and 90 WHSV for coated layer. And for 0.5% CH<sub>4</sub> is 90 WHSV in both cases.

Finally, it is compared 250 mg catalyst loading, and here it is had that for 1% CH<sub>4</sub> is 30 WHSV for kinetic and 60 WHSV for coated layer. And for 0.5% CH<sub>4</sub> is 60 WHSV in both cases.

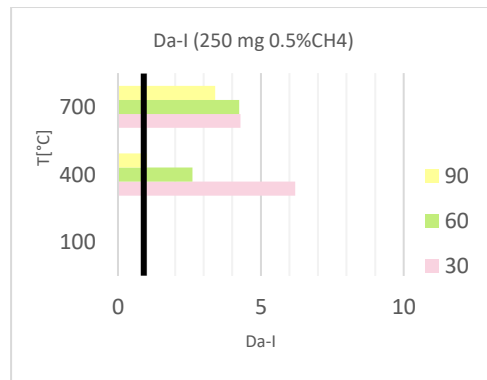
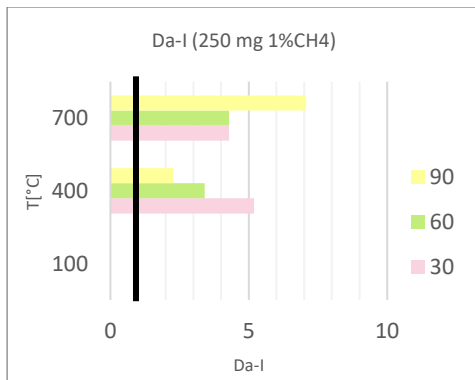
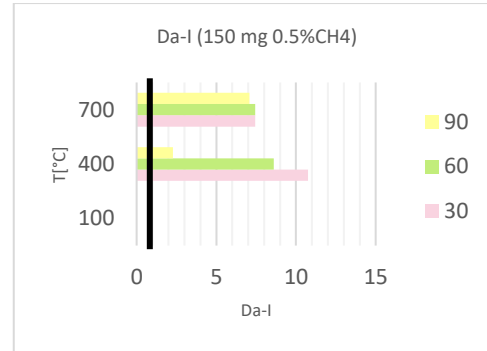
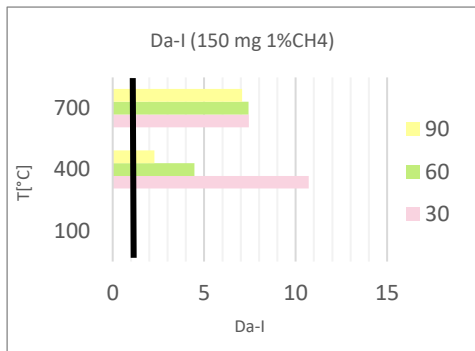
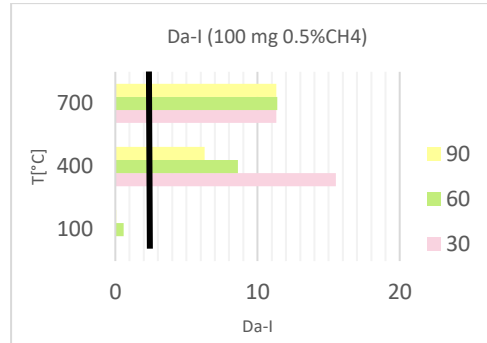
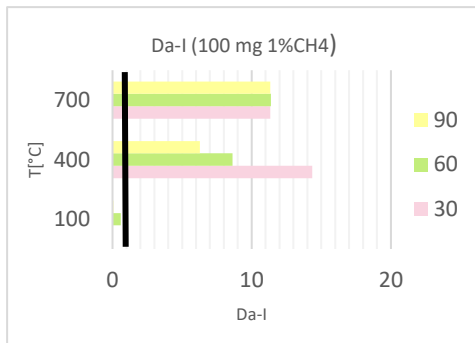
This diversity of results is because they are experimental data, on theory all activation energies should be similar, but analyzing it is verified that no.

### 11.3. Evaluation of external and internal mass transfer

#### 11.3.1. *Da-I*

1% CH<sub>4</sub>

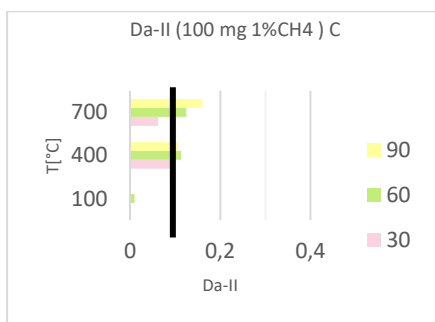
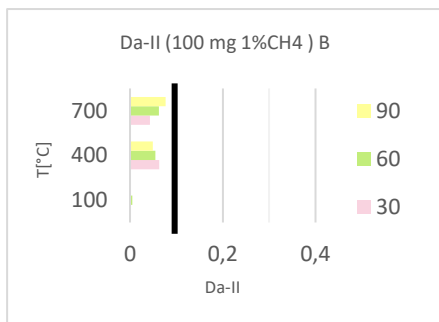
0.5% CH<sub>4</sub>



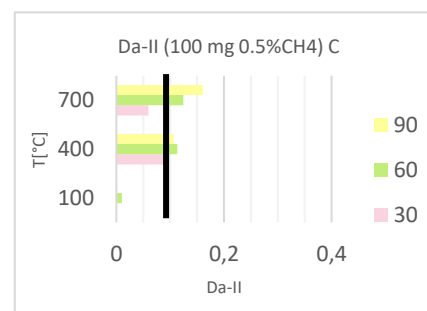
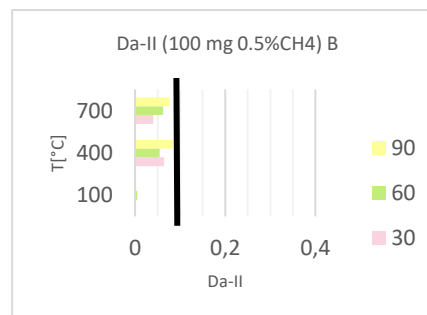
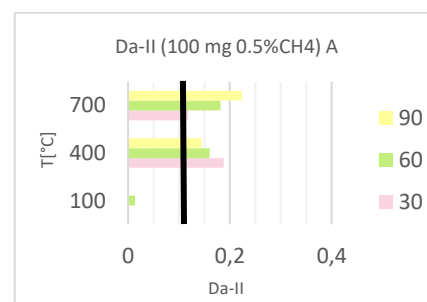
The Da-I numbers show that a temperature greater than 300 °C, it is greater than 1, so the reactant the mixture has sufficient time to react over the catalyst within OCFs pores. This happens because of high voidage of the OCF. It is also interesting to note that for the same catalyst loading (100 mg, 150 mg and 250 mg) but with different percent of CH<sub>4</sub> the Da-I numbers are similar.

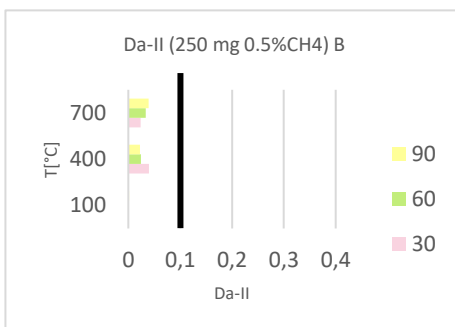
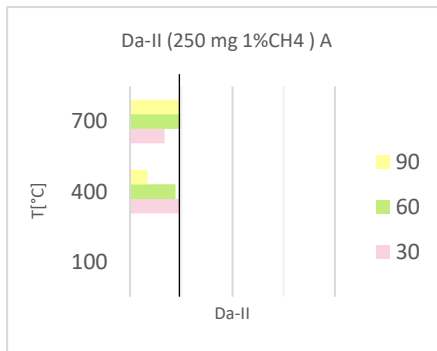
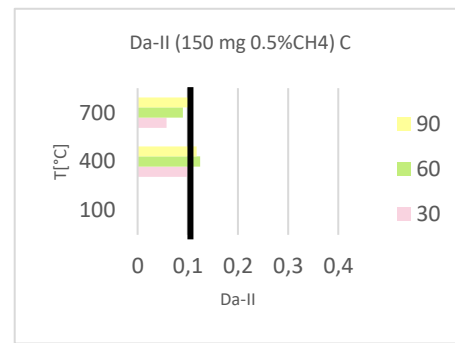
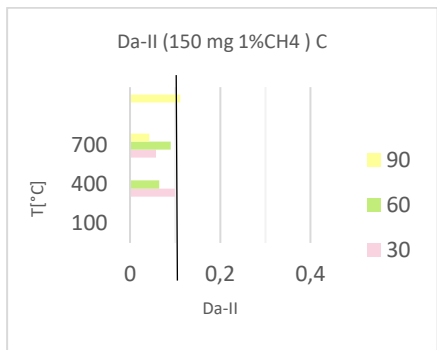
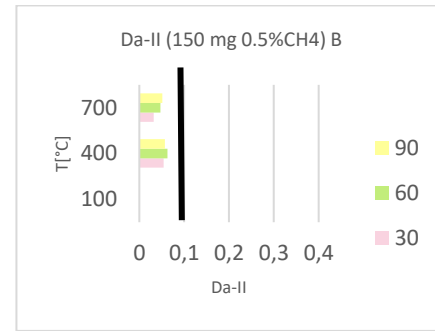
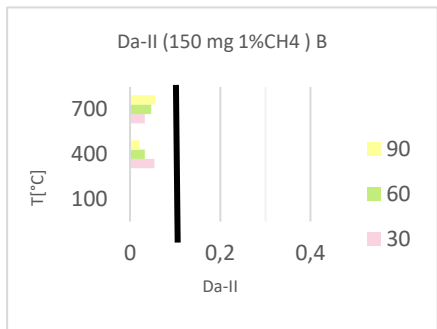
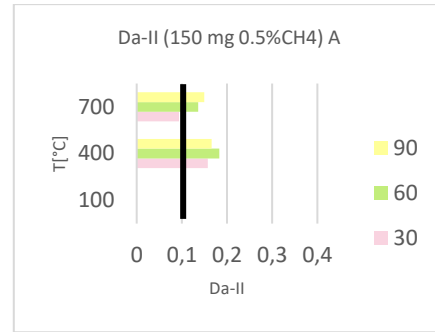
### 11.3.2. Da-II

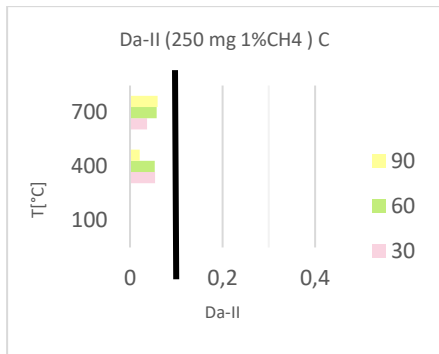
1% CH<sub>4</sub>



0.5% CH<sub>4</sub>



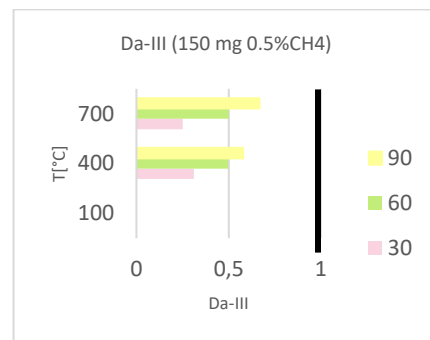
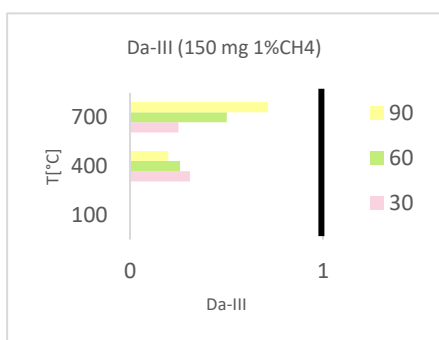
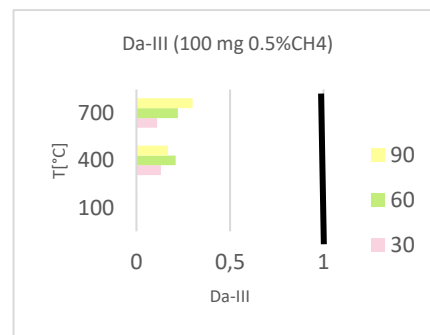
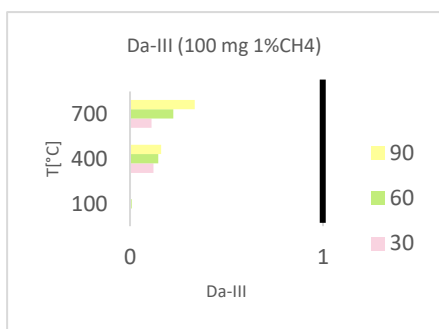




It can see that the best correlation is B, with it is achieves values lower than 0,1 in all situations. It means the absence of external diffusion limitations.

At the other correlations (A and C) when the reaction reaches temperature greater than 400 °C and the catalyst loading is 100 mg or 150 mg, Da-II is greater than 0.1 so external mass transfer limitations become important in the system.

**11.3.3. Da-III**  
 1% CH<sub>4</sub>

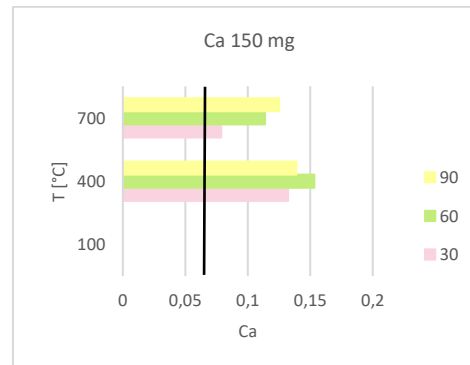
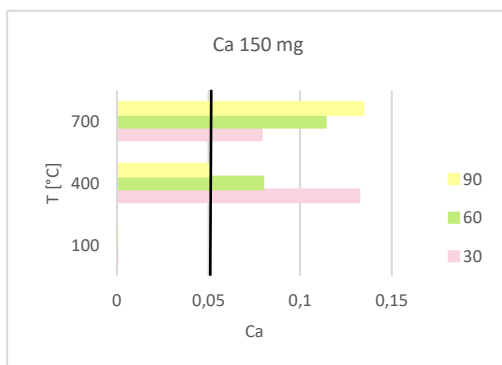
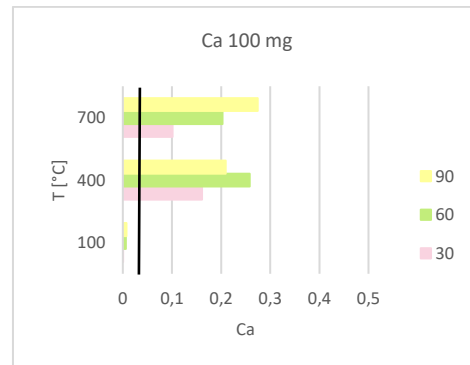
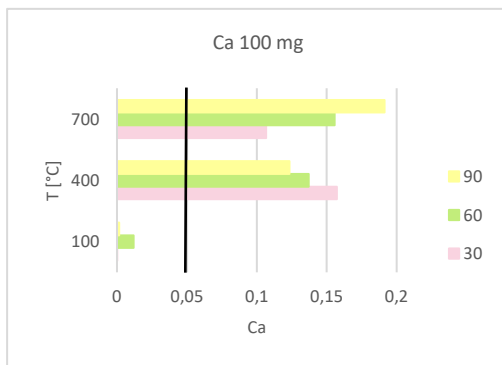


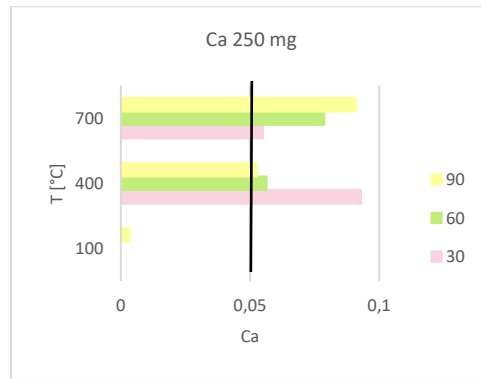
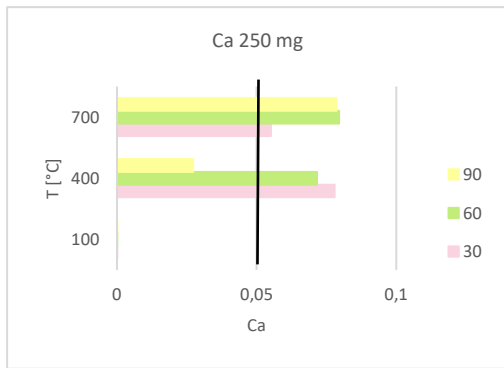
These plots show two different regimes depending on the conditions of catalyst loading and WHSV. For 100 mg and 150 mg and at any WHSV  $Da_{III}$  values are lower than 1, so there is not internal mass transfer. Thus, reactants rapidly diffuse through the pores of the coated layer, avoiding the formation of concentration gradients between the catalyst surface and active sites. However, for 250 mg is not always meet the criteria. For example, for temperatures greater than 400 and WHSV between 60 and 90,  $Da_{III}$  is greater than 1, it means that the process will have internal mass transfer because the catalyst is thicker.

#### 11.3.4. Ca

1%  $CH_4$

0.5%  $CH_4$





Here, it is only going to analyze correlation B because of it has checked that with it, external mass transfer is negligible.

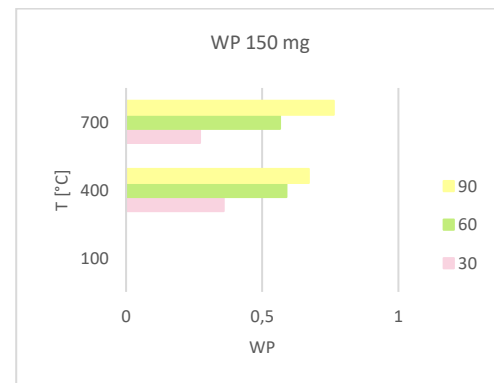
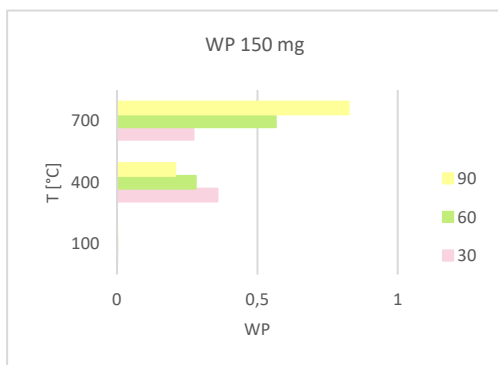
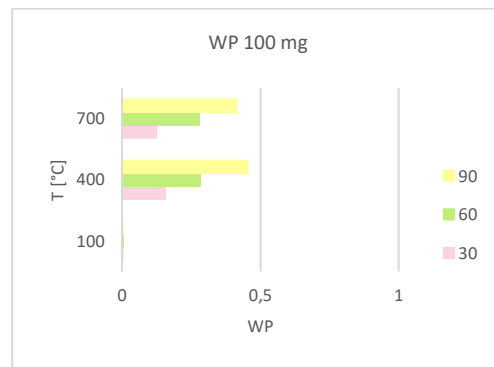
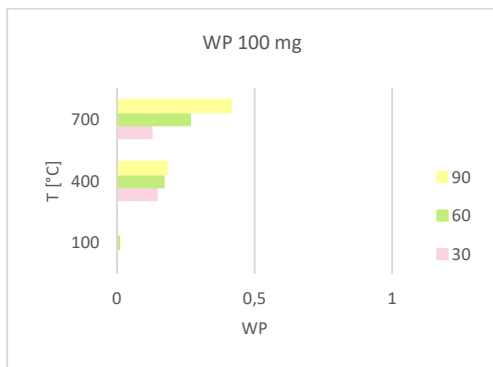
Then Carberry number is used to verify that it is right what it is said before, where this number must be less than 0.05.

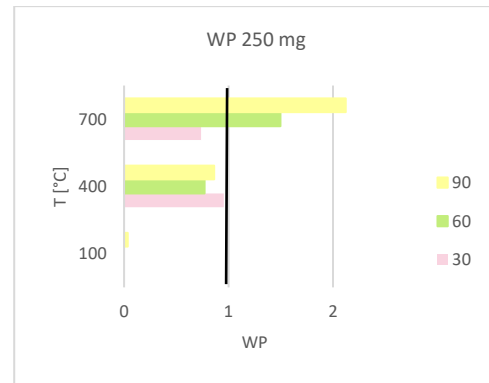
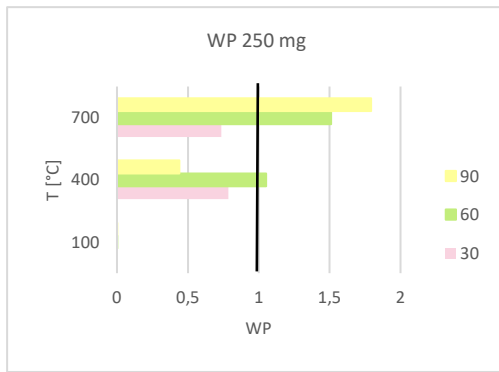
As it can see in these plots, this condition is not achieved in cases when temperatures are above 400. Therefore, would have external mass transfer. This is in contradiction with what it was said first, and it is due to Carberry number has a higher margin of error.

### 11.3.5. WP

1% CH<sub>4</sub>

0.5% CH<sub>4</sub>





The Weisz-Prater criterion is useful to confirm the results got with Da-III, here it can observe that same thing that was explained before. So, there are not internal mass transfer for 100 and 150 mg of catalyst loading.

#### 11.4. Evaluation external and internal heat transfer.

The table 10 shows that the Mears criterion was not satisfied at temperatures greater than 350°C, therefore there will be external heat transfer limitations. But these limitations will be lower when there is less methane, it is meaning for a 0.5% CH<sub>4</sub>.

**Table 10:** Mears criteria values.

		MEARS CRITERIA						
		T [°C]	1% CH <sub>4</sub>			0.5% CH <sub>4</sub>		
			100	350	700	100	350	700
100	30	0,00285216	1,22752796	0,49229119	0,0022718	0,84408157	0,25330563	
	90	0,04847274	0,70698487	1,63381412	0,05281789	0,28747134	0,49222788	
150	30	0,00541767	1,27824318	0,40972152	0	0,69041263	0,20462669	
	90	0,00797774	0,19395534	0,76027789	0	0,2717062	0,54343515	
250	30	0,00052949	0,63568586	0,3579862	0	0,59313074	0,20269662	
	90	0,00118876	0,14663828	0,65147805	0,04787316	0,1330114	0,33115549	

**Table 11:** Anderson criteria values.

		ANDERSON CRITERIA						
		T [°C]	1% CH <sub>4</sub>			0.5% CH <sub>4</sub>		
			100	350	700	100	350	700
100	30	6,82E-09	5,70E-06	5,61E-06	5,54E-09	4,01E-06	2,94E-06	
	90	1,19E-07	3,41E-06	1,90E-05	1,29E-07	1,37E-06	5,69E-06	
150	30	3,21E-08	1,47E-05	1,15E-05	0,00E+00	7,93E-06	5,73E-06	
	90	4,89E-08	2,31E-06	2,19E-05	0,00E+00	3,24E-06	1,56E-05	
250	30	1,43E-08	3,36E-05	4,57E-05	0,00E+00	2,54E-05	2,57E-05	
	90	3,35E-08	8,04E-06	8,44E-05	1,34E-06	7,22E-06	4,43E-05	

As it can be seen in table 11, the values are much lower than 0.75, so the temperature gradients inside the catalytic coating can be neglected, according to Anderson criteria. This is because the extremely thin coating layer.

### 11.5. Resistance to mass transfer

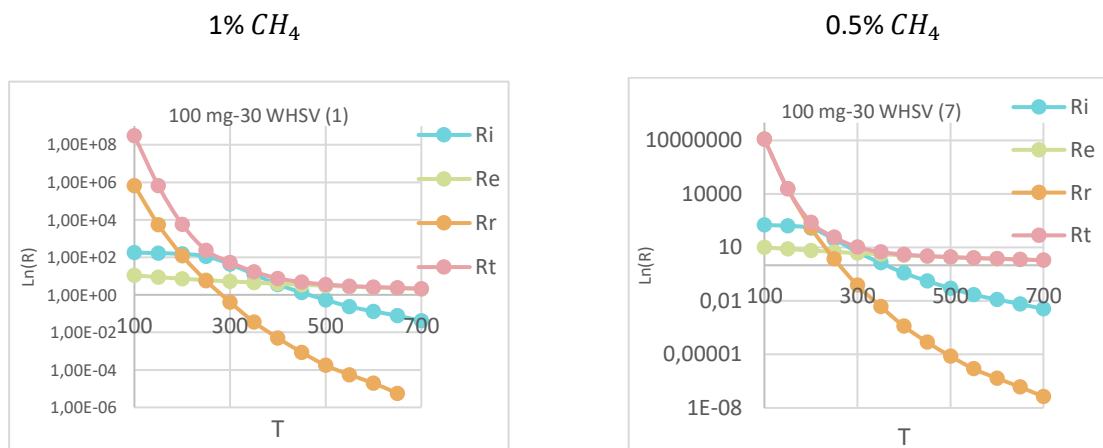
As it was said in the section 8, there are different regimes depending on temperature, washcoat and fluid phase properties, catalyst loading, channel dimensions and WHSV. These regimes include kinetic regime (KR), transition regime-1 (TR-1), washcoat diffusion controlled regime (WD), transition regime-2 (TR-2) and external mass transfer regime (ER).

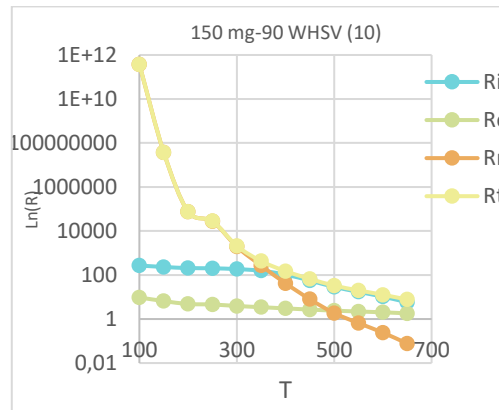
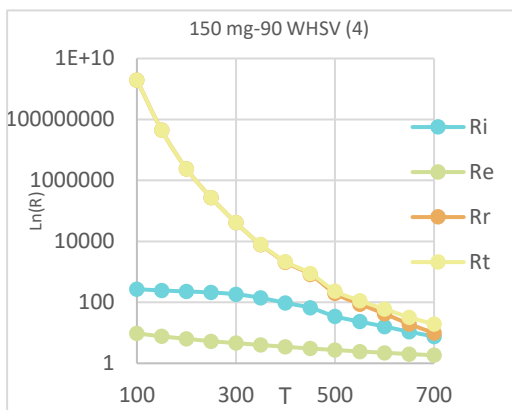
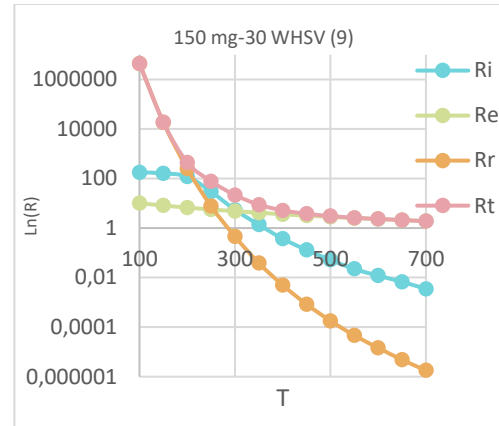
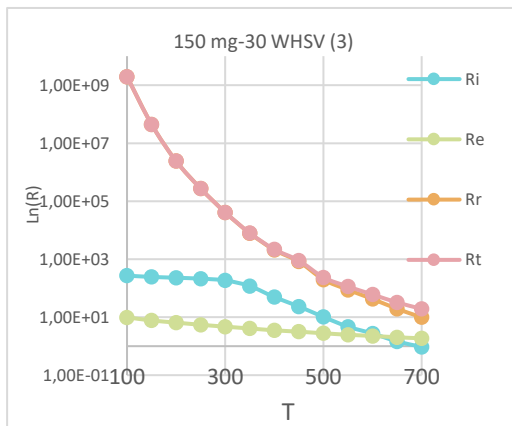
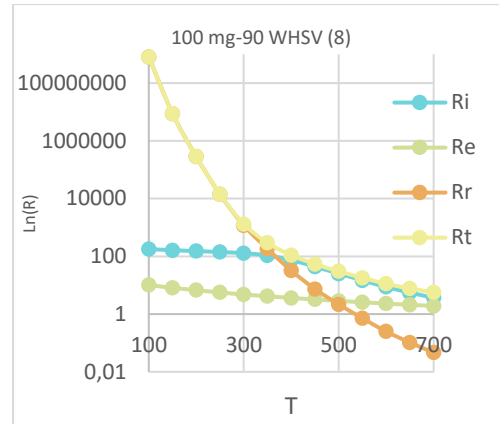
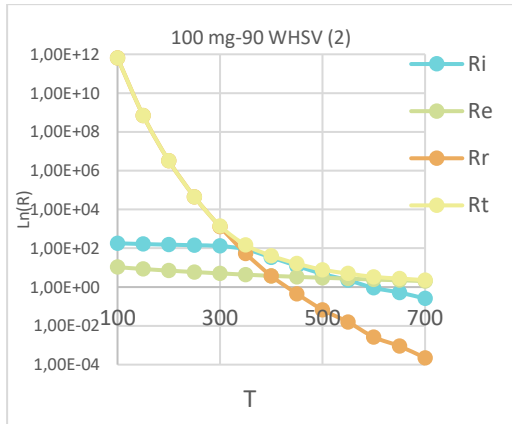
Firstly, it will explain theoretically what happens in each regime, but then it will observe that they are not occurred in all cases.

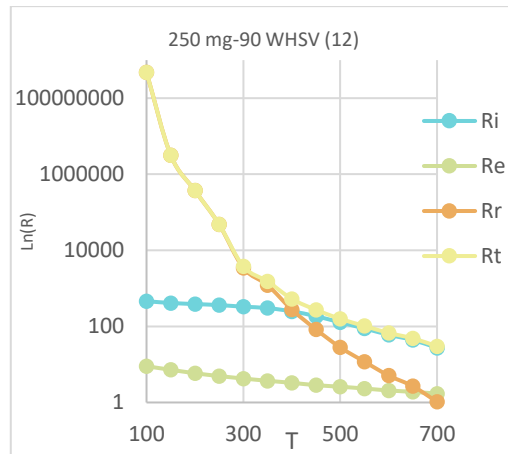
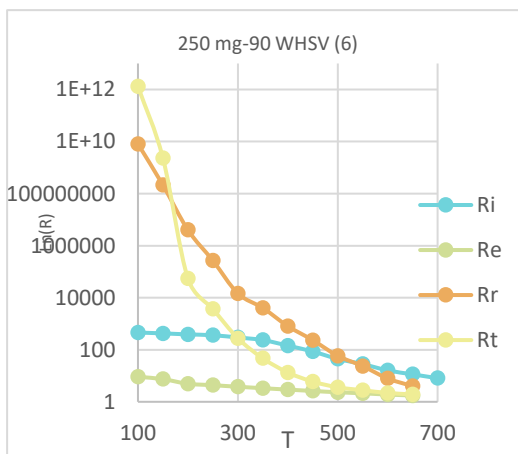
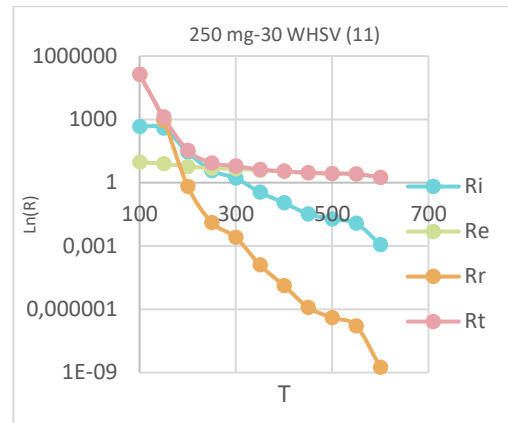
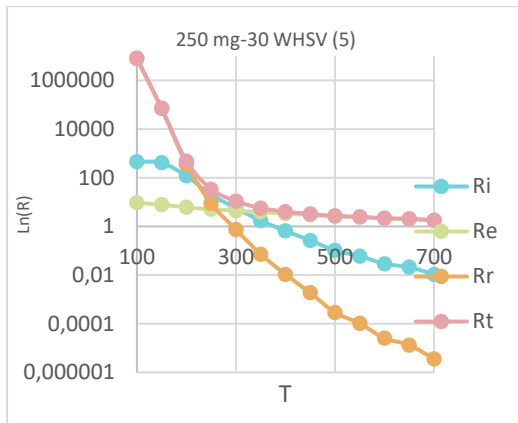
1. Kinetic regime: At low temperatures the reaction rate is much slower than the rate of external mass transfer and internal diffusion. The reaction happens across the washcoat and a nearly uniform concentration profile is observed in the transverse direction in the OCF. In this regime holds that  $R_r \gg (R_i + R_e)$  and  $C_{fm} \approx C_s \approx C$ .
2. Transition regime-1: The temperature is increased therefore the reaction rate too and the concentration in the washcoat decreases. The diffusional limitations begin to appear, but the external mass transfer is negligible compared to the reaction resistance. Here  $C_{fm} \approx C_s$ .
3. Washcoat diffusion controlled regime: In this regime the characteristic time for internal diffusion ( $t_{int}$ ) is much greater than reaction and external mass transfer time ( $t_r$  and  $t_{ext}$  respectively). Here  $R_i \gg (R_r + R_e)$  and  $C \ll C_s, C_{fm} \approx C_s$ .
4. Transition regime-2: At this moment the reaction rate increases exponentially following the Arrhenius equation and the external mass transfer limitations begins to appear. Here  $C \ll C_s$ .
5. External mass transfer controlled regime: Finally, at high temperature, the characteristic reaction time is closer to zero and the reactant concentration drops to a small value. Strong inter- and intra-phase concentration gradients prevail ( $C_s \ll C_{fm}$  and  $C \ll C_s$ ) Hence in this regime the process depends on the external mass transfer. Here  $R_e \gg (R_r + R_i)$

In the following analysis will be studied these regimes in five different ways where the behavior will be observed at 30 and 90 WHSV, being the best and the worst space velocity respectively.

#### 11.5.1. Resistance Vs. Temperature.







These plots show the relation of the three individual resistance ( $R_e$ ,  $R_i$ ,  $R_r$ ) and the overall resistance with temperature. It can appreciate that each resistance decreases with temperature, excluding external mass transfer resistance which is almost independent of temperature.

Mainly, at low temperature ( $T < 350^\circ\text{C}$ ) reaction resistance controls the process (KR), meanwhile at high temperatures ( $T > 500^\circ\text{C}$ ) is the external resistance (ER). At intermediate temperature ( $350^\circ\text{C} < T < 500^\circ\text{C}$ ) the internal resistance is the largest (WD).

This explanation can be perfectly observed in plot 2, 5, 7 and 11, where pink or yellow (according to WHSV) line coincide with blue, green or orange line (depending on resistance).

However, reaction resistance controls the system for cases 3 and 4, as it can be seen on them.

### 11.5.2. Concentration ratios Vs. Temperature

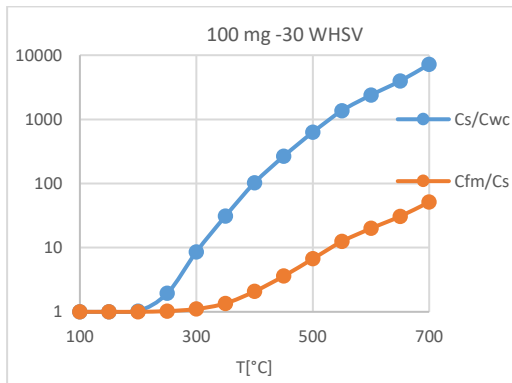
To classify different regimes in OCF, it is used these equations at steady state and for first order kinetics,

$$\frac{C_s}{C} = 1 + \frac{R_i}{R_r} \quad (84)$$

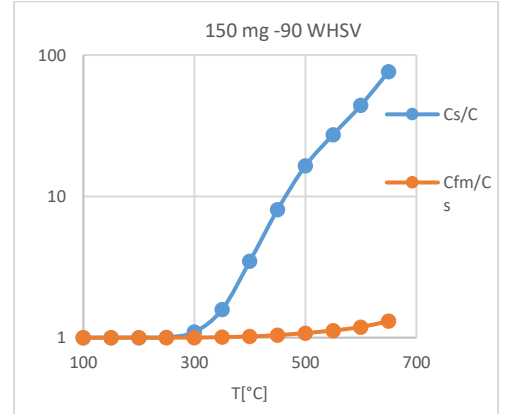
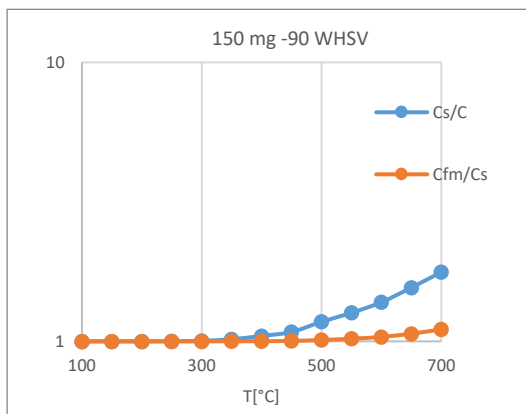
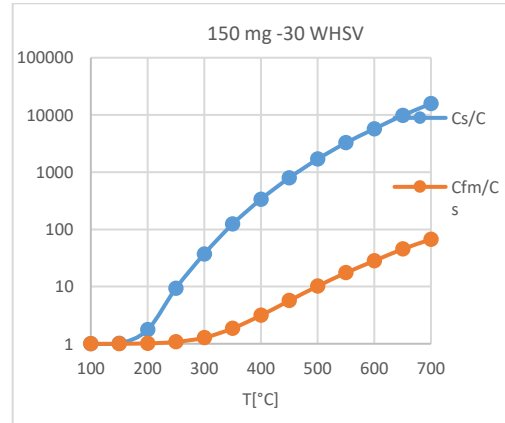
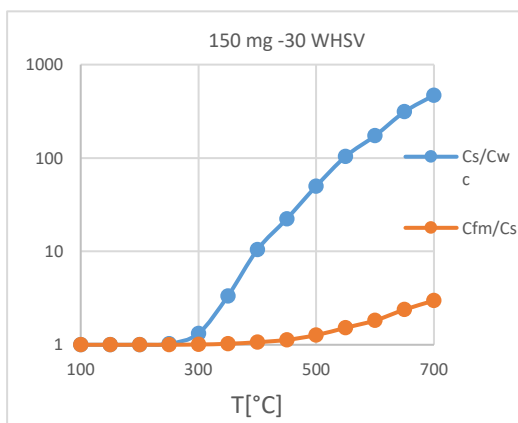
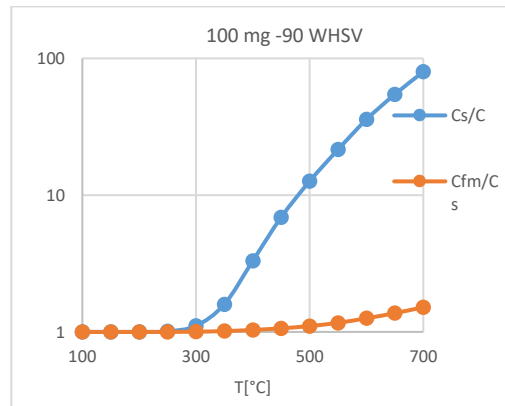
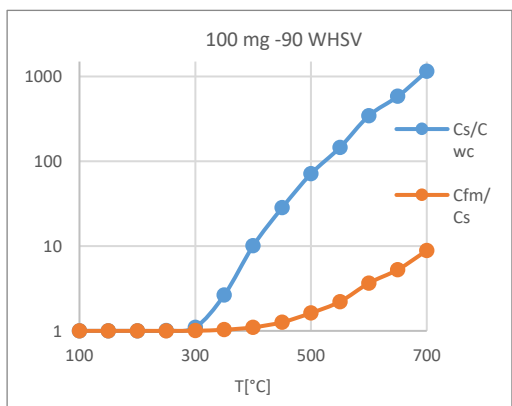
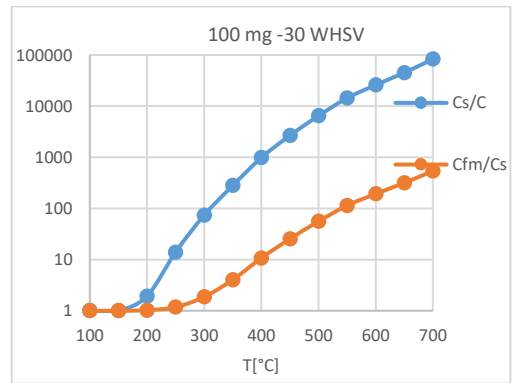
$$\frac{C_{fm}}{C_s} = \frac{R_t}{R_w + R_r} \quad (85)$$

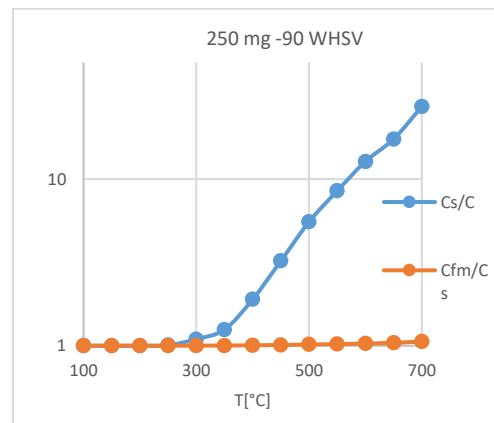
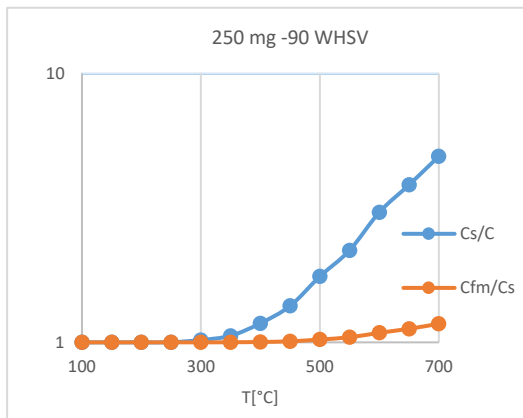
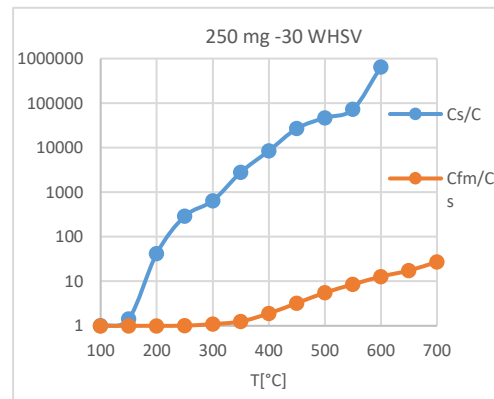
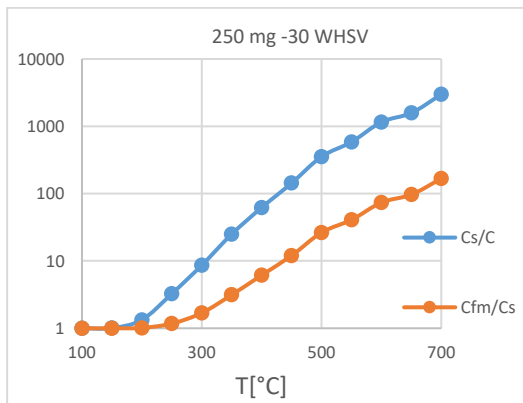
Particularly, they are useful in determining the regime transition. For instance, in the kinetic regime, almost uniform concentration profile predominates ( $C_{fm} \approx C_s \approx C$ ), meanwhile in the mass transfer controlled regime, more accentuated concentration gradients is seen that in the other case ( $\frac{C_s}{C} \gg 1$  and  $\frac{C_{fm}}{C_s} \gg 1$ ).

1% CH<sub>4</sub>



0.5% CH<sub>4</sub>





Here it can be seen that for temperatures lower than 350 °C the concentration ratios approach unity, therefore the reaction resistance controls the process. As temperature increases (350°C < T < 500°C), diffusional limitations start to appear in the washcoat diffusion regime (WD). At T > 500°C the OCF works in a mass transfer controlled regime in which the external mass transfer resistance is dominant. Hence, it is confirmed what it was said in the previous plots.

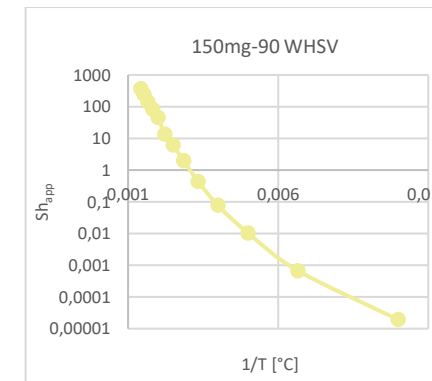
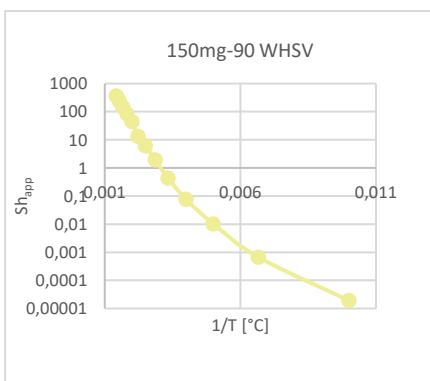
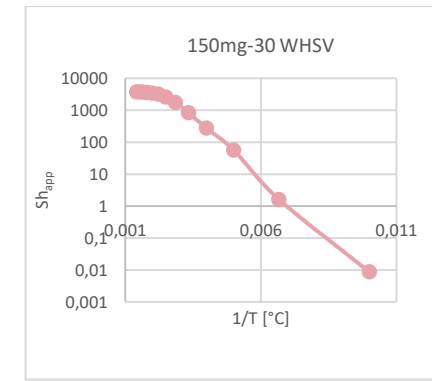
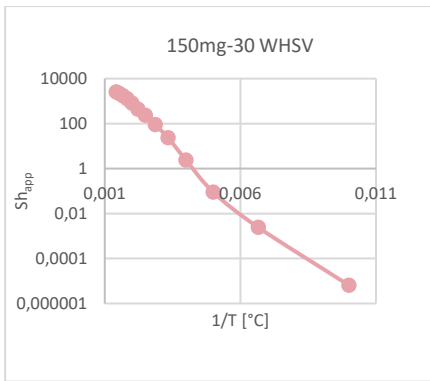
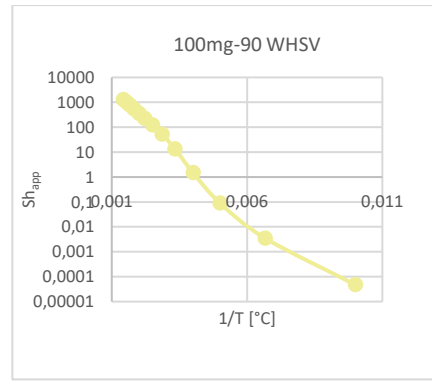
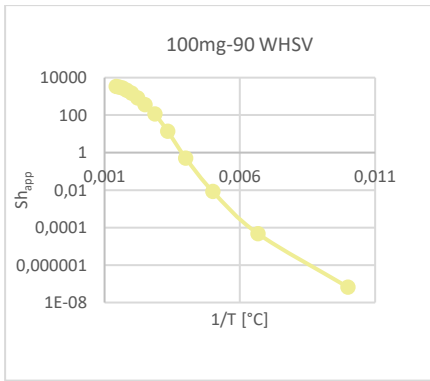
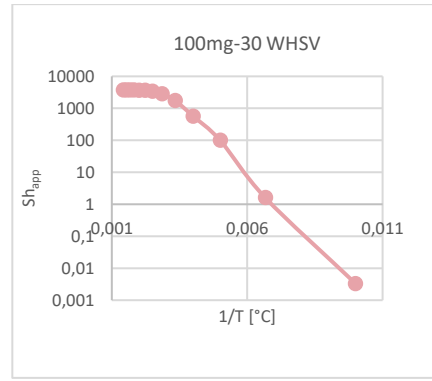
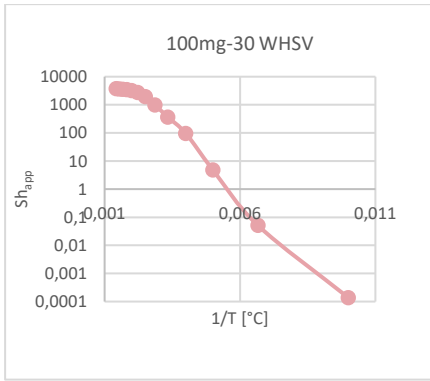
### 11.5.3. $Sh_{app}$ vs. $\frac{1}{T}$

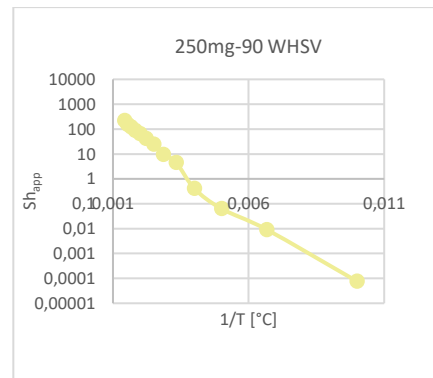
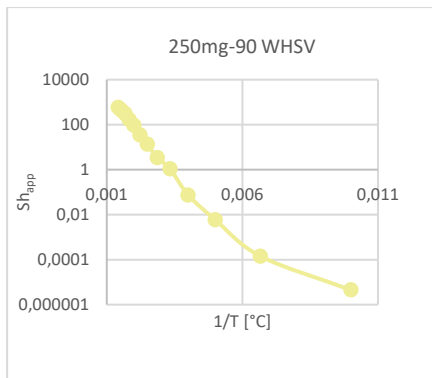
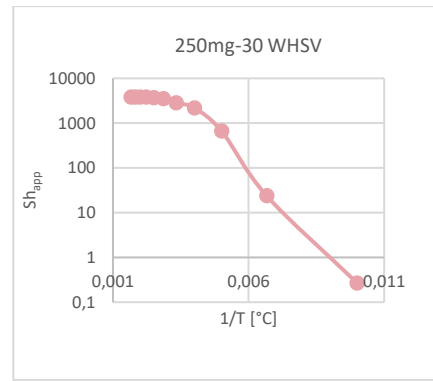
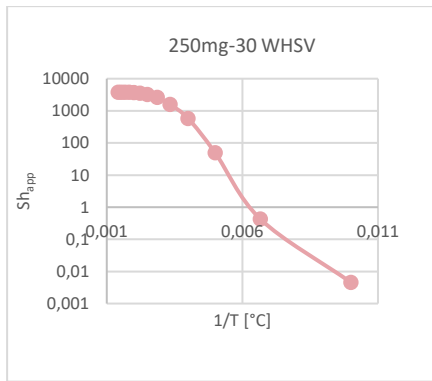
Below is presented another way to determine the regimes where is plotting experimentally observable overall Sherwood number with the inverse of temperature. This number is calculated by the following equation:

$$Sh_{app} = \frac{4km_{app}R_{\Omega 1}}{D_M} \quad (86)$$

1%  $CH_4$

0.5%  $CH_4$





In these plots, it can appreciate that  $Sh_{app}$  approaches the asymptote begins to appear external mass transfer, meaning ER regime. This is observed specially in the cases of 30 WHSV.

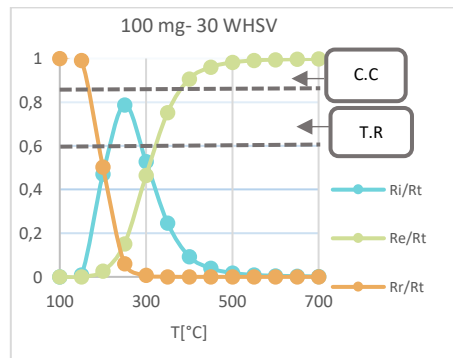
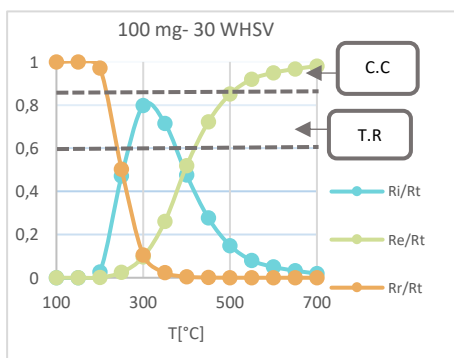
#### 11.5.4. External, internal or reaction resistance/ total resistance ratio Vs. Temperature.

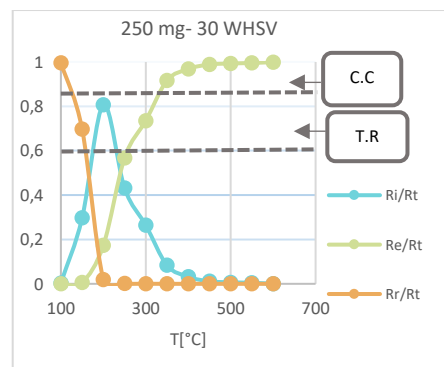
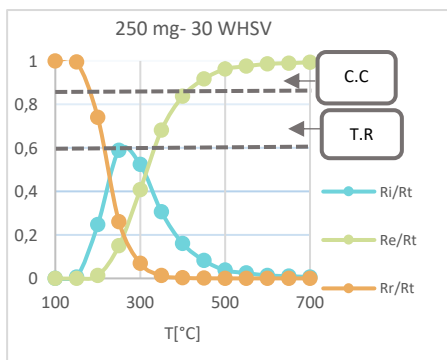
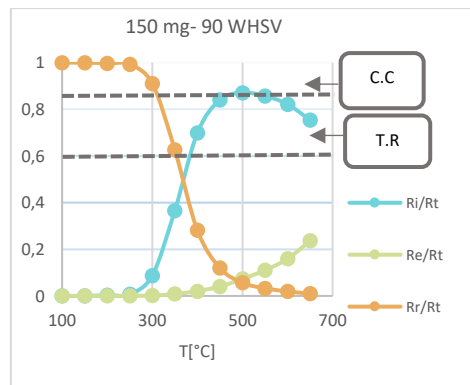
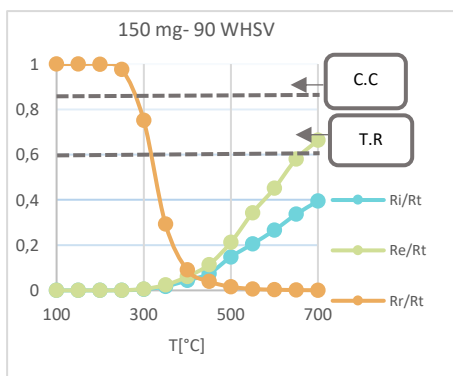
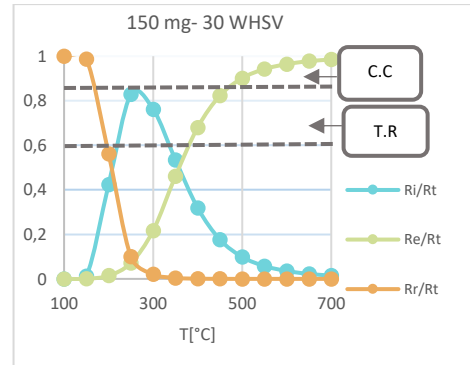
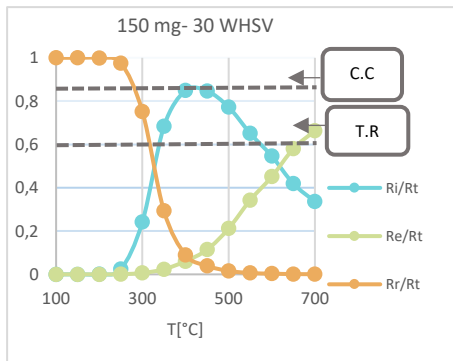
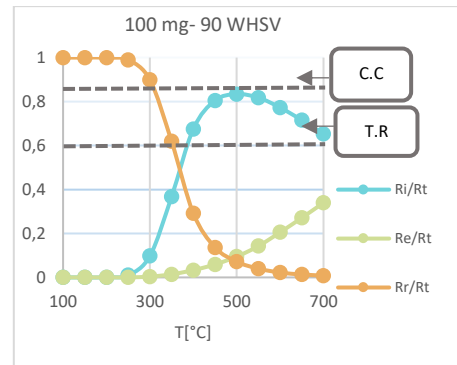
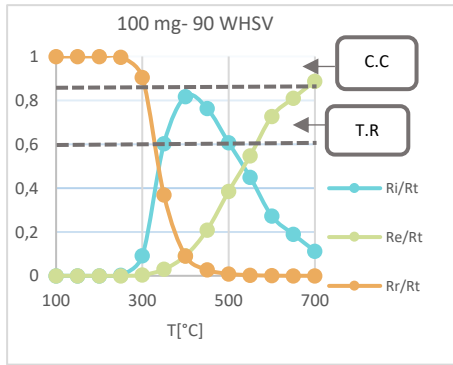
Another analysis to study mass transfer is the following:

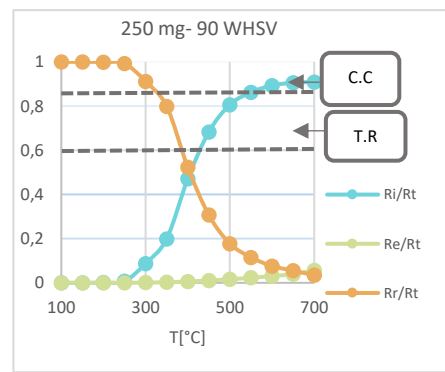
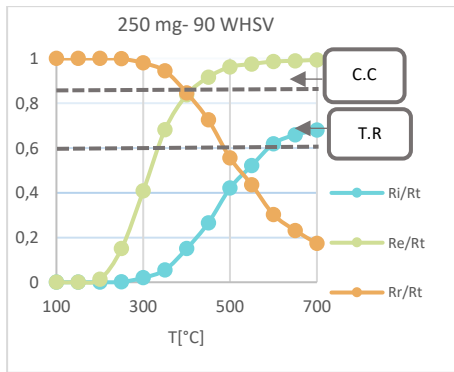
when the value is greater than 0.85 is known that the process is completely controlled (C.C.) and when it is found between 0.6 to 0.85 the process is in transition regime (T.R.)

1%  $CH_4$

0.5%  $CH_4$







Looking the plots, it is seen on them that internal resistance is never found in area of completely controlled. And reaction resistance is always under control at low temperature.

### 11.5.5. Effectiveness factor Vs. Modulus Thiele.

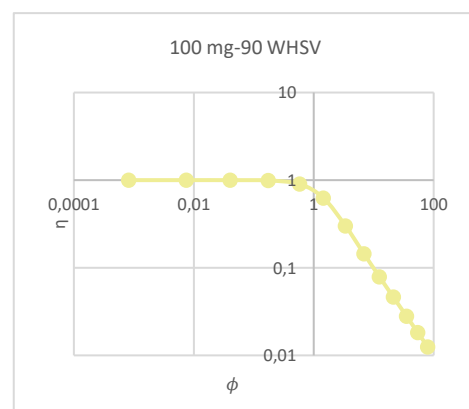
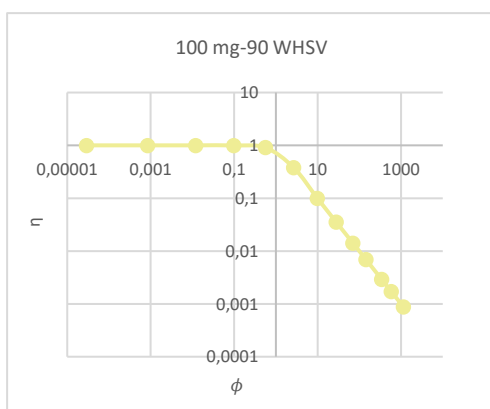
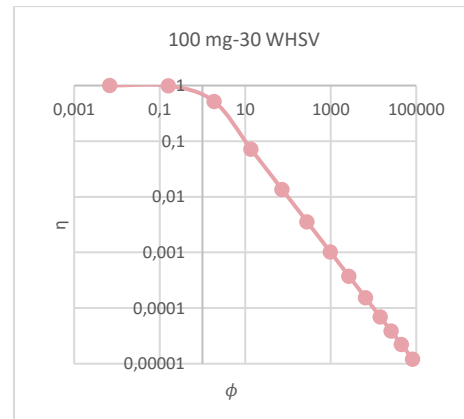
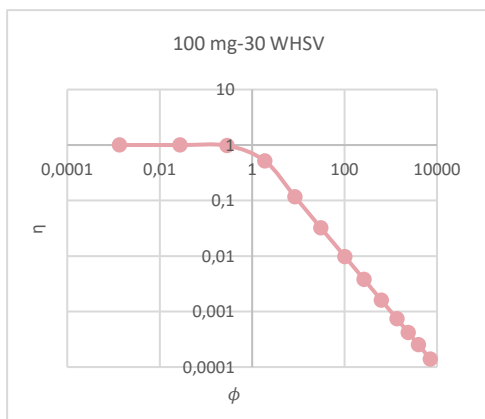
Before to analyze the plots, it is necessary to know the effectiveness factor has two asymptotes:

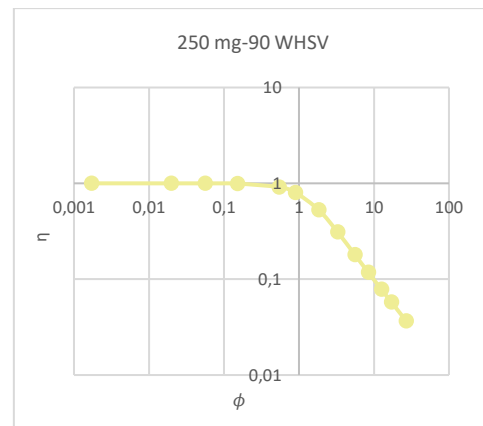
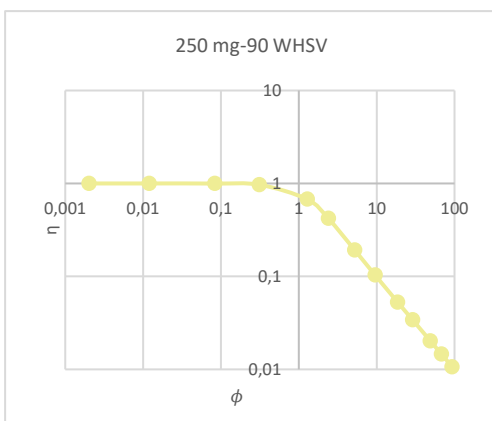
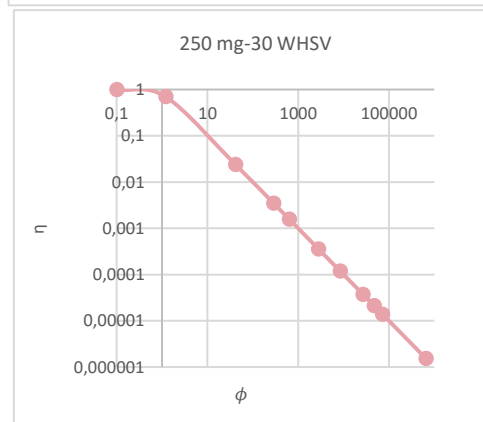
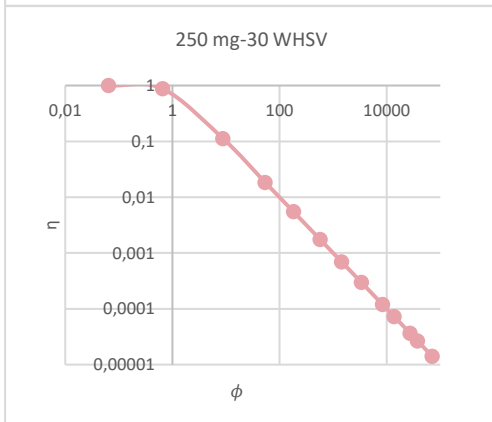
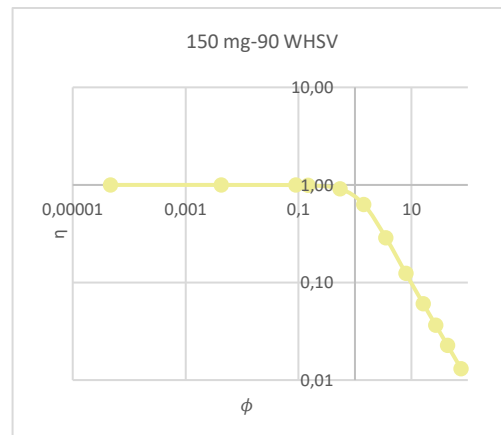
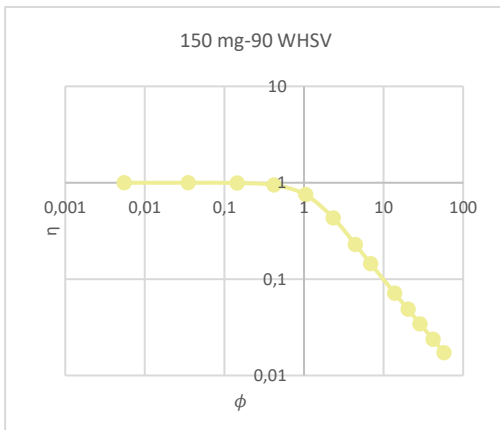
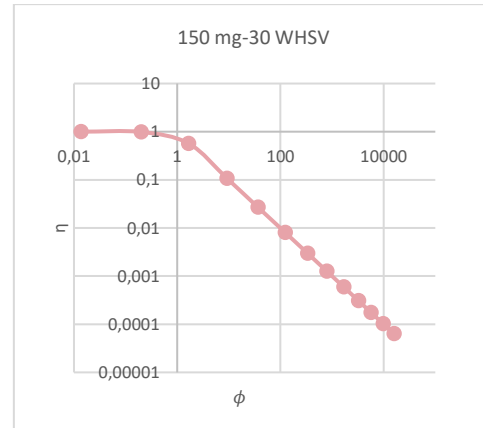
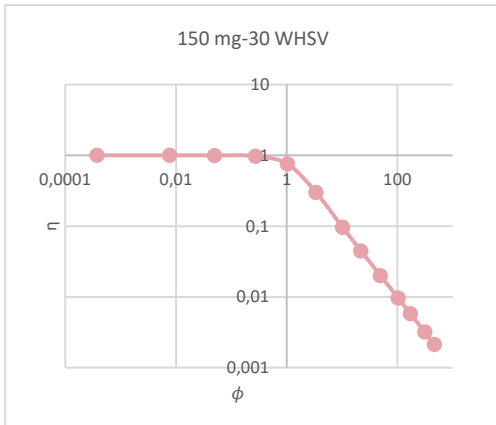
Slow reaction:  $\eta \rightarrow 1$  and  $\phi \ll 1$

Fast reaction:  $\eta \rightarrow 1/\phi$  and  $\phi \gg 1$

1% CH<sub>4</sub>

0.5% CH<sub>4</sub>





At the beginning, effectiveness factor tends to be 1, so the course of the reaction will be slow, as temperature increases, effectiveness factor decreases due to Thiele modulus increases and hence, the reaction will be faster. This can observe in all cases.

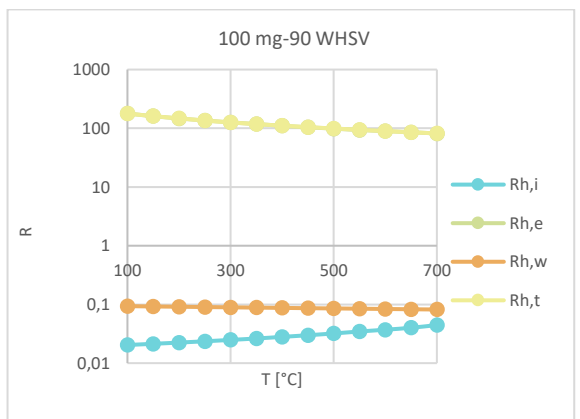
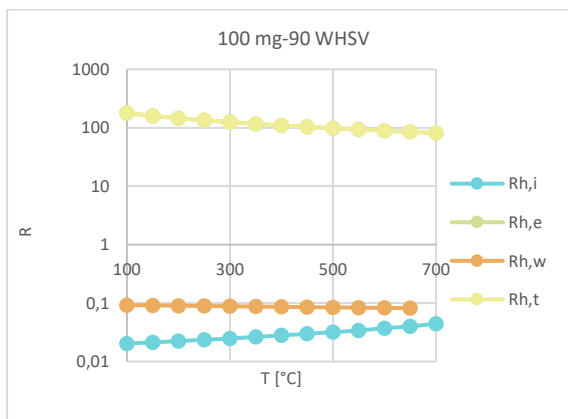
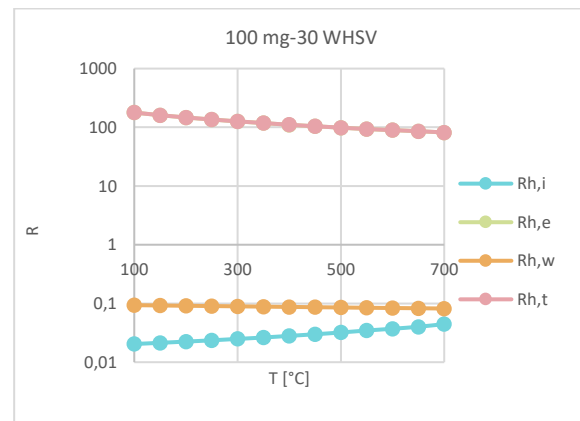
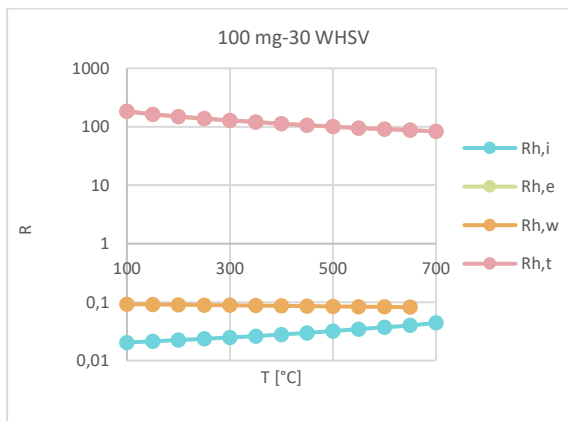
### 11.6. Resistance to heat transfer

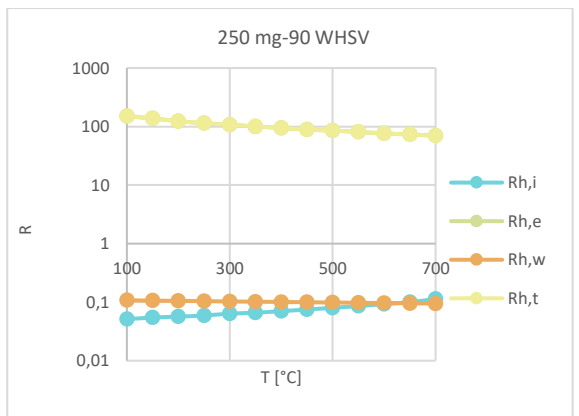
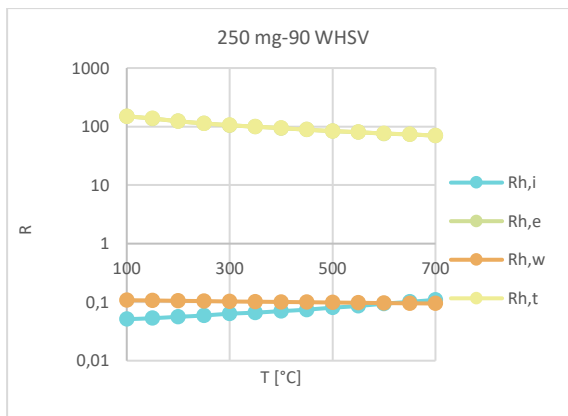
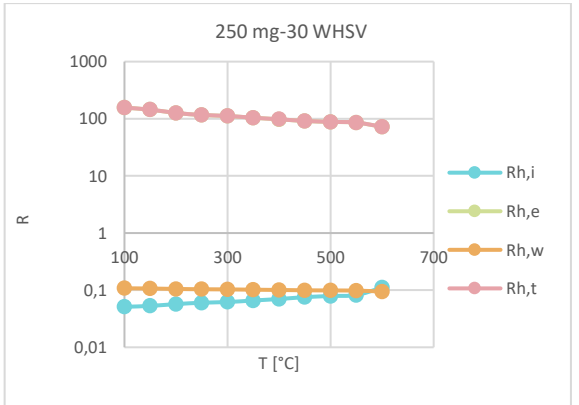
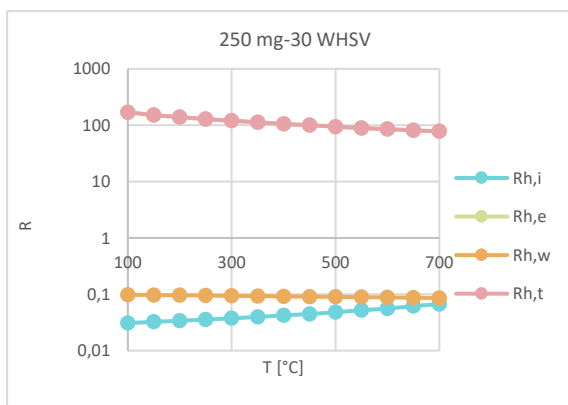
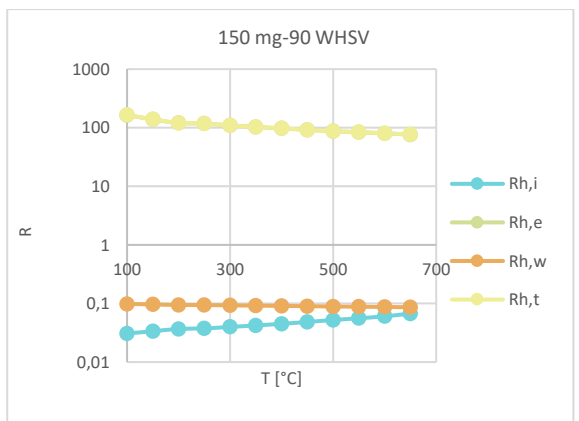
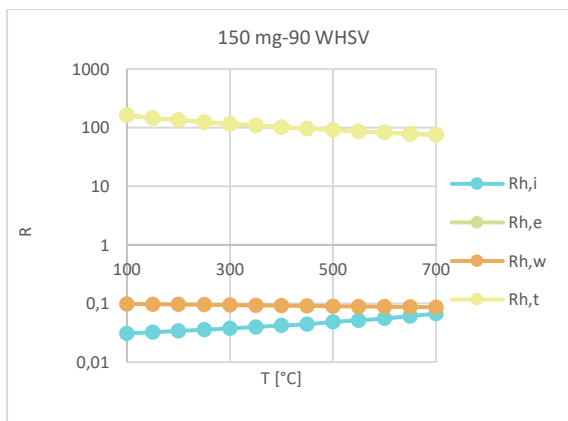
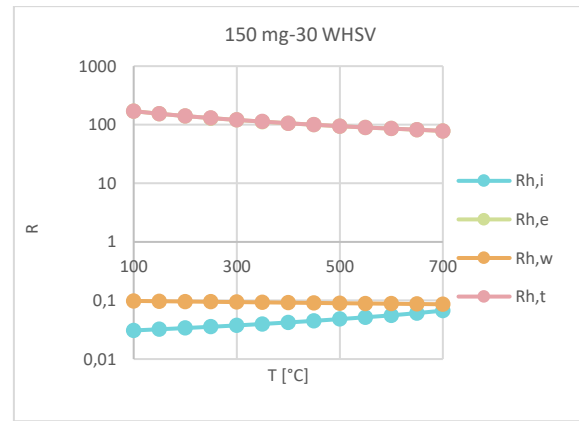
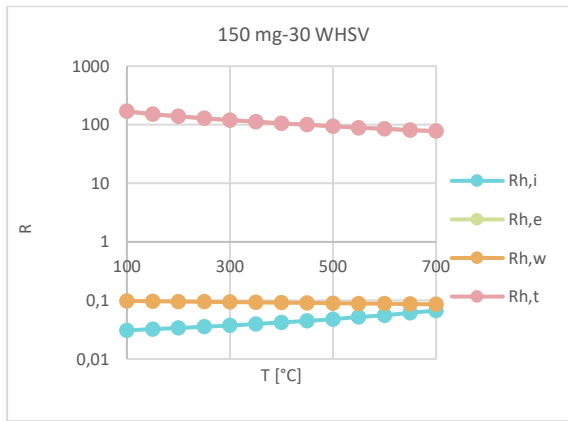
In order to study resistance to heat transfer, it will discuss three types of plots below. All information related to how to calculate the resistance and dimensionless numbers you can find in section 9. As in the study of mass transfer, it will analyze 30 and 90 WHSV.

#### 11.6.1 Heat transfer resistance Vs. Temperature

1%  $CH_4$

0.5%  $CH_4$





In these plots it can observe that external resistance is the largest due to thermal conductivity of mixture is the lowest conductivity compared to Zirconia and cobalt oxide. On the other hand, the internal

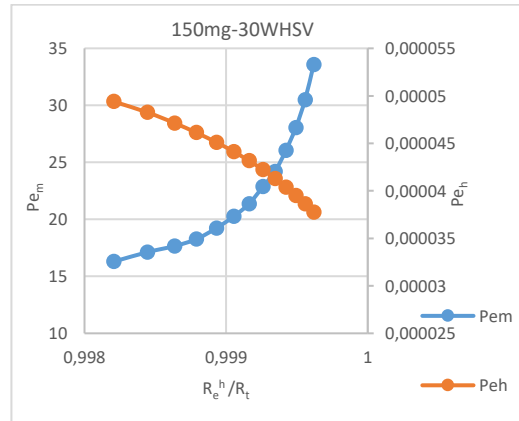
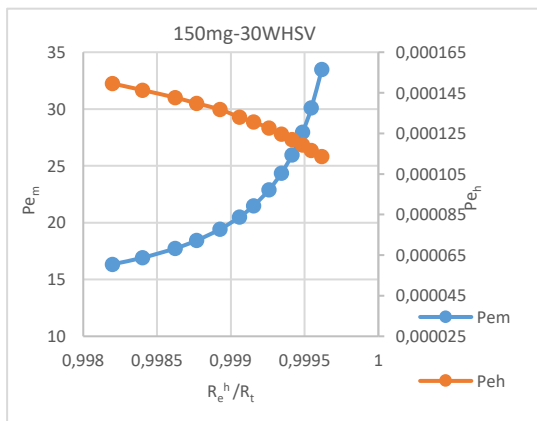
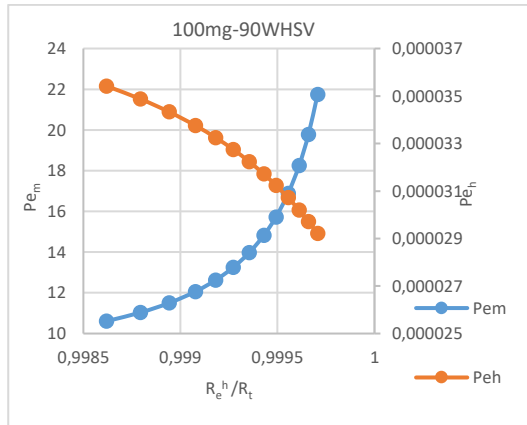
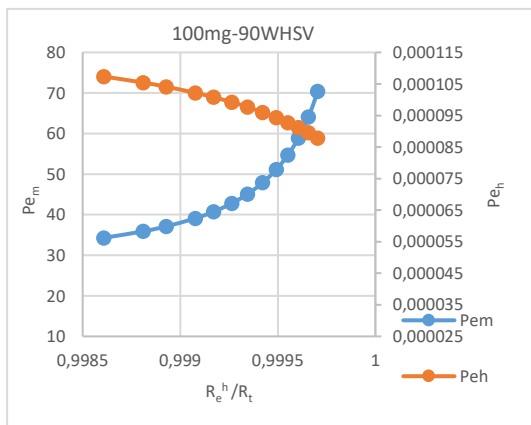
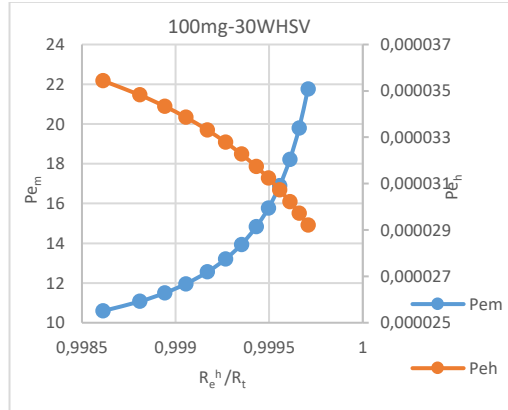
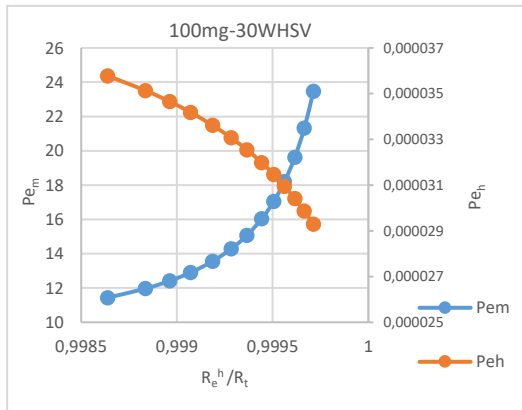
resistance has the lowest values, it means that cobalt oxide is the component that transfers the most heat.

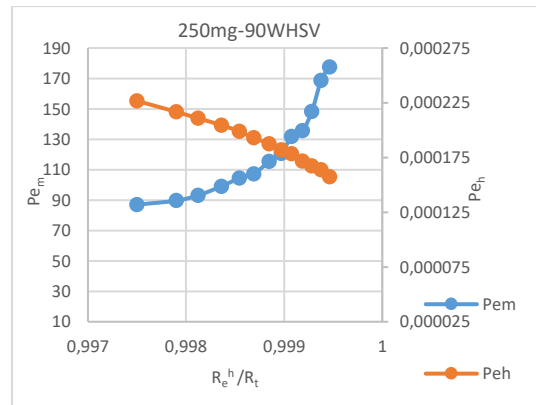
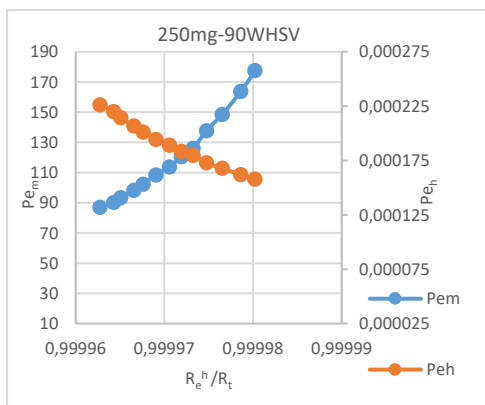
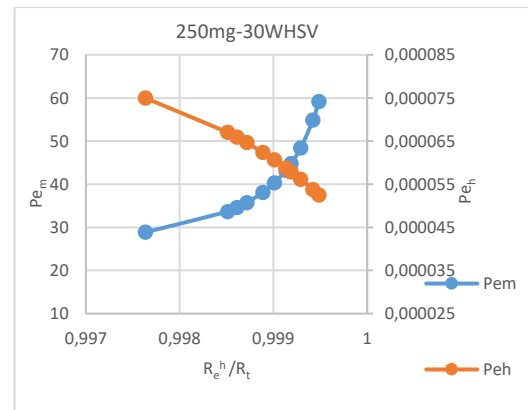
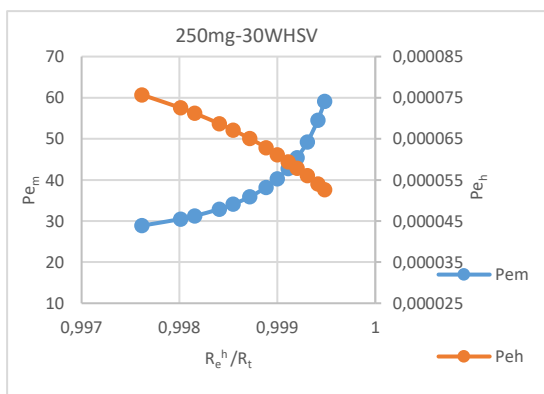
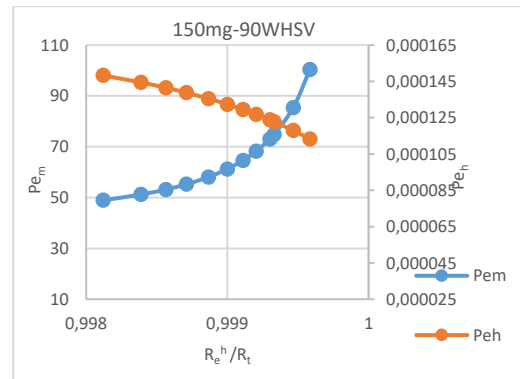
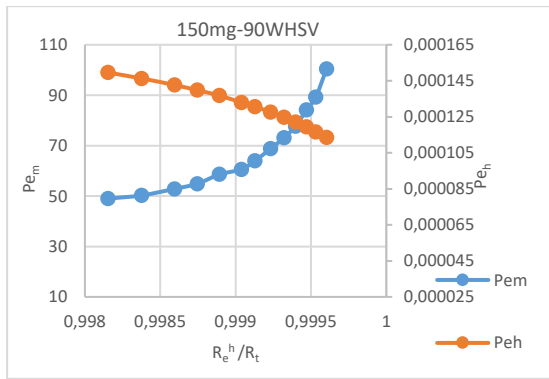
Also, it can tell that both internal and wall resistance have the same values for each catalyst loading because they do not depend on space velocity.

**11.6.2. Peclet numbers Vs. external resistance/total resistance ratio**

1% CH<sub>4</sub>

0.5% CH<sub>4</sub>

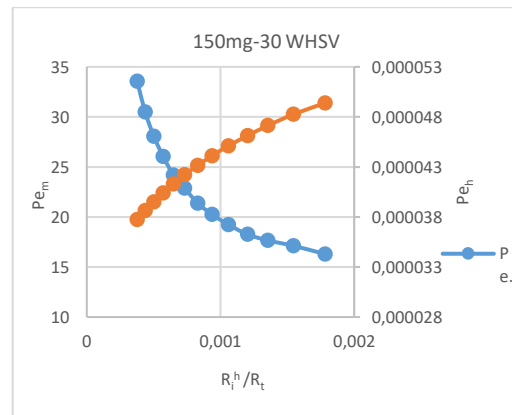
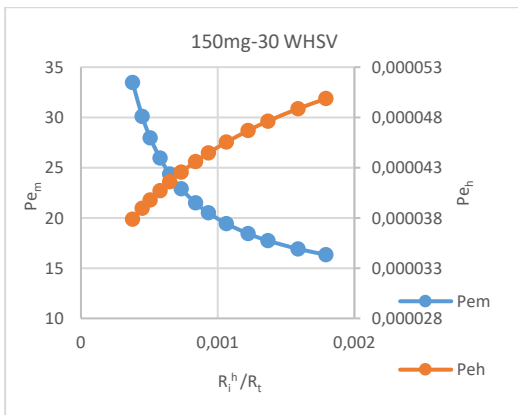
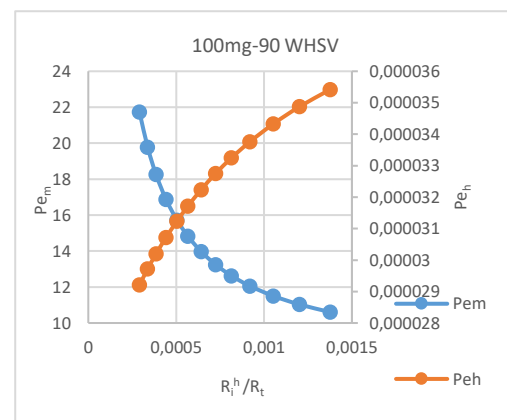
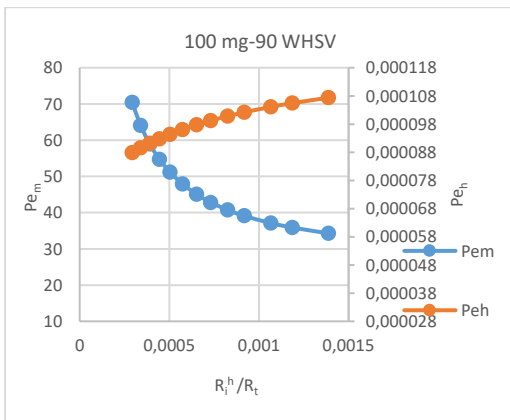
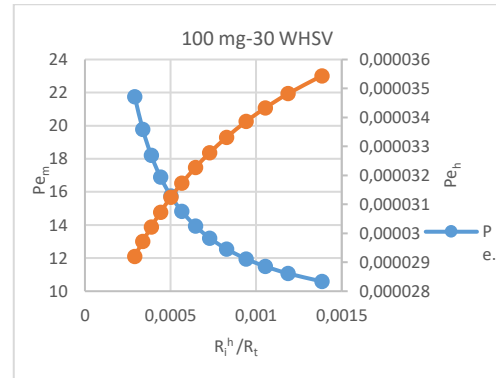
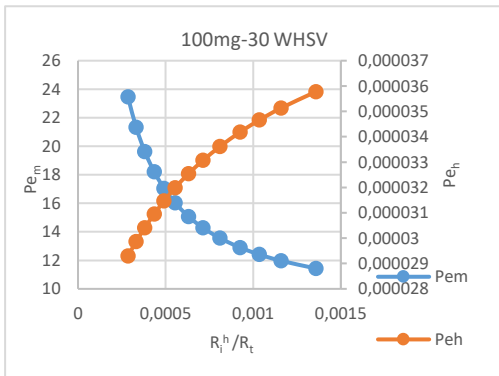


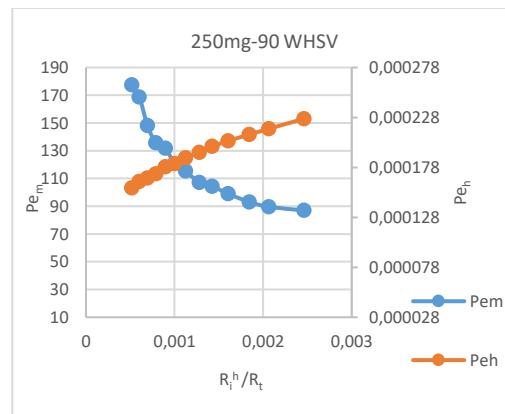
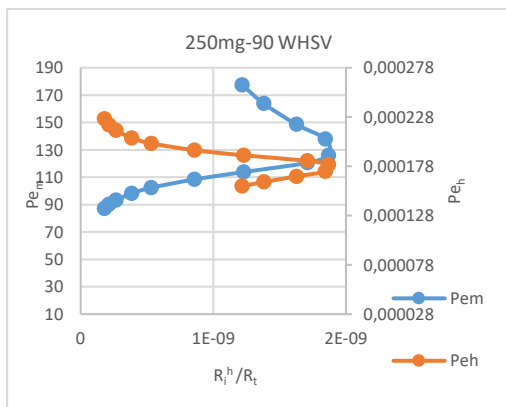
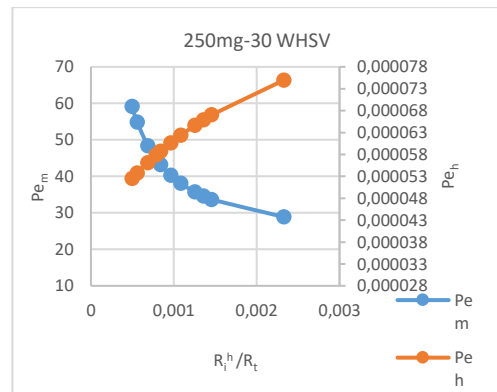
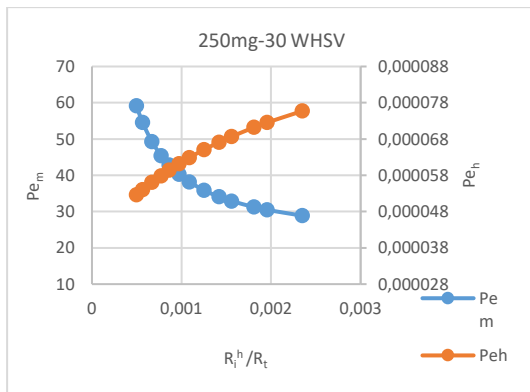
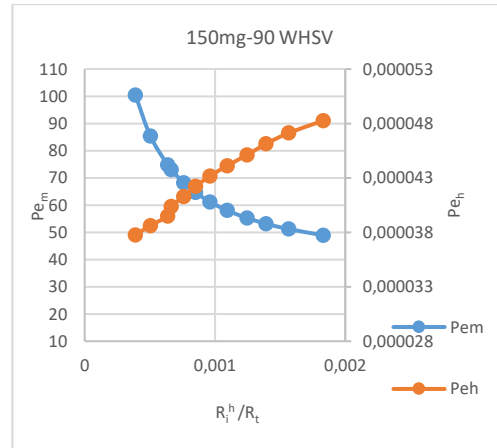
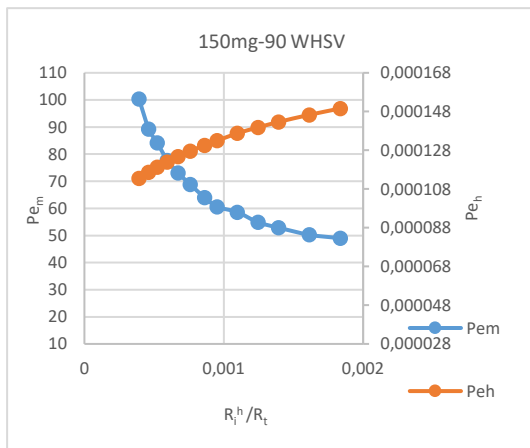


**11.6.3. Peclet numbers Vs. internal resistance/total resistance ratio**

1% CH<sub>4</sub>

0.5% CH<sub>4</sub>





Both types of plots follow the same behavior, where the mass Peclet number is always much larger than heat Peclet number. It is also important to consider that at higher temperatures, mass and heat are dispersed.

Also, it is important to discuss that if it is compared the data for 1% CH<sub>4</sub> to 0.5 % CH<sub>4</sub> there is no appreciable difference.

### 11.7. Estimation of mass transfer coefficient.

In order to estimate the correlation is necessary to take the points from conversions equal to and greater than 50 % until the complete control of mass transfer. This usually happens in a range between 400°C to 600°C more or less. And estimate molecular diffusion (Section 3), Schmidt (Section 5) and Sherwood numbers for that temperature range. Sherwood number is determined by this equation,

$$Sh = \frac{k_m d_{p,c}}{D_M} \quad (86)$$

Where  $k_m$  is the mass transfer coefficient, and it is defined with the following equation,

$$k_m = \frac{-\ln(1 - X_{CH_4})Q}{V_{cat}S_{ag}} \quad (87)$$

Once they have been calculated all data, it is used the least squares method, which is a standard approach in regression analysis to approximate the solution of overdetermined systems.

$$\begin{aligned} \sum \text{Log}Y &= \text{Log}\alpha \cdot N + \beta \cdot \sum \text{Log}X \\ \sum \text{Log}X \cdot \text{Log}Y &= \text{Log}\alpha \cdot \sum \text{Log}X + \beta \cdot \sum (\text{Log}X)^2 \\ Y &= \alpha \cdot X^\beta \end{aligned}$$

By this method it is obtained one correlation for internal mass transfer (1), which is calculated from 50% of conversion until to the point at which the transformation from palladium to palladium oxide begins. And another for the external mass transfer (2), which is estimated from the points at which the transformation is initiated until the complete control of mass transfer. Which are shown below,

$$Sh = 0.28 * Sc^{\frac{1}{3}} * \left( Re \frac{d_p}{L} \right)^{0.07} \quad (88)$$

$$Sh = 1.63 * Sc^{\frac{1}{3}} * \left( Re \frac{d_p}{L} \right)^{0.07} \quad (89)$$

Finally, the correlation is as follows,

$$Sh = 1.91 * Sc^{\frac{1}{3}} * \left( Re \frac{d_p}{L} \right)^{0.07} \quad (90)$$

## 12. Conclusion

In order to finish the work, the following conclusions are briefly summarized:

1. From a conversion point of view, both 100 mg 1% and 0.5% 30 WHSV are the best options to achieve full methane conversion in a temperature range between 400 and 600.
2. With Damköhler numbers are observed that the mixture has sufficient time to react inside OCF pores in all cases.  $Da-II$  is also useful to know that the B is the best correlation and there are no external diffusion limitations for any case but analyzing Carberry number you can see that if. And finally, with last number  $Da-III$ , it shows that the best choices are 100 or 150 mg catalyst loading where there is not internal mass transfer, and this is checked with WP as well.
3. The criteria used to determine resistance to mass transfer allow to know the transition temperatures between the regimes as a function of various operating variables. The case that the best fits the theoretical explanation is for 100 mg and 30 WHSV due to longer contact time (both methane concentrations), being at the beginning reaction resistance the dominant one, at intermediate temperature internal resistance and at high temperatures external resistance. It has also combined the various resistance to obtain an experimentally observable overall mass transfer coefficient ( $Sh_{app}$ ), which allow to observe perfectly external mass transfer at 30 WHSV. This is because by increasing the greater space speed is movement of the reacting gas molecules, which leads to a decrease in the external mass transfer.
4. Regarding to resistance to heat transfer, Cobalt oxide is the component that transfers the most heat because of it has the highest conductivity value. The external resistance is the only one that varies in all cases since it depends on the space velocity. In all cases, the expected behavior is followed. And when comparing the plots obtained for different methane concentrations it is seen that they are almost equal.

### 13. Bibliography

- [1] Catalytic Performance of Pd/Co<sub>3</sub>O<sub>4</sub> on SiC and ZrO<sub>2</sub> Open Cell Foams for the Process Intensification of Methane Combustion in Lean Conditions. G. Ercolino, P. Stelmachowski, S. Specchia. 2017.
- [2] Rh/CeO<sub>2</sub> Thin Catalytic Layer Deposition on Alumina Foams: Catalytic Performance and Controlling Regimes in Biogas Reforming Processes. C. Italiano, M. A. Ashraf, L. Pino, C. W. Moncada Quintero, S. Specchia and A. Vita. 2018. DOI:10.3390/catal8100448.
- [3] The Effect of the Preparation Method of Pd-Doped Cobalt Spinel on the Catalytic Activity in Methane Oxidation Under Lean Fuel Conditions. G. Ercolino, A. Grodzka, G. Grzybek, P. Stelmachowski, S. Specchia, A. Kotarba. 2016. DOI: 10.1007/s11244-016-0620-0.
- [4] Handbook of Combustion Vol.5: New Technologies. S. Specchia, E. Finocchio, G. Busca and V. Specchia. 2010. ISBN:978-3-527-32449-1.
- [5] Speciation-controlled incipient wetness impregnation: A rational synthetic approach to prepare sub-nanosized and highly active ceria-zirconia supported gold catalysts. E. Rio, D. Gaona, J. C. Hernández-Garrido, J. J. Calvino, M. G. Basallote, M. J. Fernández-Trujillo, J. A. Pérez-Omil, J. M. Gatica. 2014. DOI: 10.1016/j.jcat.2014.07.001.
- [6] Algunos métodos para la estimación de la viscosidad. Available in: <http://tecno.cruzfierro.com/formularios/viscosidad>.
- [7] Chapter 11. Example 11.1: Prediction of Binary Gas Diffusivities. University of Michigan. 2007. Available in: <http://www.umich.edu/~elements/fogler&gurmen/html/course/lectures/eleven/exam4.htm>
- [8] R. H. Perry, D. W. Green, Perry's chemical engineers' handbook, The McGraw-Hill Companies, 1999.
- [9] M. Bracconi, M. Ambrosetti, M. Maestri, G. Groppi, E. Tronconi. Analytical Geometrical Model of Open Cell Foams with Detailed Description of Strut-Node Intersection. 2017.
- [10] M. Bracconi, M. Ambrosetti, M. Maestri, G. Groppi, E. Tronconi, A fundamental investigation of gas/solid mass transfer in open-cell foams using a combined experimental and CFD approach, Chemical Engineering Journal (2018). DOI: <https://doi.org/10.1016/j.cej.2018.07.023>.
- [11] Calculating heat of combustion. Polymer Science Learning Center. 2019. Available in: <https://pslc.ws/fire/cellulos/combcals.htm>
- [12] Overall mass transfer coefficients and controlling regimes in catalytic monoliths. J. Saurabh, M. Harold, V. Balakotaiah. 2009. DOI: 10.1016/j.ces.2009.11.021
- [13] Determination of Kinetics and controlling regimes for H<sub>2</sub> oxidation on Pt/Al<sub>2</sub>O<sub>3</sub> monolithic catalyst using high space velocity experiments. J. Saurabh, M. Harold V. Balakotaiah. 2010. DOI: 10.1016/j.apcatb.2010.12.030.
- [14] Impact of heat and mass dispersion and thermal effects on the scale-up of monolith reactors. T. Gu and V. Balakotaiah. 2015. DOI: 10.1016/j.cej.2015.09.005.
- [15] 2.3.7 Thermal conductivities. National Physical Laboratory. 2017. Available in: [http://www.kayelaby.npl.co.uk/general\\_physics/2\\_3/2\\_3\\_7.html](http://www.kayelaby.npl.co.uk/general_physics/2_3/2_3_7.html)
- [16] Co<sub>3</sub>O<sub>4</sub> nanostructures: the effect of synthesis conditions on particles size, magnetism and transport properties. P. Sahoo, H. Djieutedjeu and P. Poudeu. 2013. DOI: 10.1039/c3ta13442c.